

UNCLASSIFIED
~~CONFIDENTIAL~~

6
Copy
RM E55G14

NACA RM E55G14

UNCLASSIFIED



RESEARCH MEMORANDUM

ANALYTICAL COMPARISON OF CONVECTION-COOLED TURBINE
BLADE COOLING-AIR REQUIREMENTS FOR SEVERAL
RADIAL GAS-TEMPERATURE PROFILES

By James E. Hubbarth and Henry O. Slone

Lewis Flight Propulsion Laboratory
Cleveland, Ohio

*7 sep
copy of RA-12.9 Effective Date 7/11/58
JSD*

~~CONFIDENTIAL~~

SEP 11 1955

LANGLEY AERONAUTICAL LABORATORY
RESEARCH TRIANGLE PARK, VIRGINIA

CLASSIFIED DOCUMENT

This material contains information affecting the National Defense of the United States within the meaning of the espionage laws, Title 18, U.S.C., Secs. 793 and 794, the transmission or revelation of which in any manner to an unauthorized person is prohibited by law.

NATIONAL ADVISORY COMMITTEE
FOR AERONAUTICS

WASHINGTON

September 7, 1955

To UNCLASSIFIED

CLASSIFICATION CHANGED

~~CONFIDENTIAL~~
UNCLASSIFIED

NATIONAL ADVISORY COMMITTEE FOR AERONAUTICS

RESEARCH MEMORANDUMANALYTICAL COMPARISON OF CONVECTION-COOLED TURBINE BLADE COOLING-AIR
REQUIREMENTS FOR SEVERAL RADIAL GAS-TEMPERATURE PROFILES

By James E. Hubbartt and Henry O. Slone

SUMMARY

An analysis has been made to permit a comparative evaluation of the turbine rotor cooling-air requirements with convection-cooled blades for the following four combustor-outlet radial gas-temperature profiles along the blade span: (1) a uniform profile, (2) a profile representable by a complete cycle of the cosine wave using the cooler gas layers near the turbine casing and stator inner ring and a hot gas core, (3) a profile representable by one-half cycle of the cosine wave using the cooler gas layers near the stator inner ring and the hotter gas layers near the turbine casing, and (4) an optimum profile resulting in the absolute minimum cooling-air requirements. In each case, the cooling-air-flow requirements are compared with profile (1), which has been used in turbine-cooling analyses. This uniform profile can be obtained only at the expense of combustor pressure drop or length or both. Profiles (2) and (3) are obtainable from present combustor designs that have good performance. These profiles have the advantage of either eliminating or decreasing the turbine casing and stator-ring cooling problems at elevated temperatures, profile (2) being better in this respect.

The results indicate that, for turbine design root stresses of 25,000 psi and turbine-inlet temperatures near 2600° R (conditions of immediate interest), profile (2) requires turbine rotor coolant flows slightly higher than those of the uniform profile for flight Mach numbers near 2.0 with blade-inlet cooling-air temperatures near 1000° R. For a Mach number near 2.5, the coolant flow for this condition might be increased by 35 percent. For higher stresses, profile (2) becomes less favorable on the basis of coolant-flow requirements, but profile (3) becomes more favorable. A reduction in coolant flow of 20 percent for turbine designs applicable to conditions of immediate interest may be obtained by using profile (4). This 20-percent change in coolant flow would probably be reflected in approximately a 1-percent change in thrust and horsepower of turbojet and turboprop engines. Profile (4), however, exposes the stator inner ring to the hottest gas layers and may present an extreme inner-ring cooling problem.

3776

T-80

INTRODUCTION

The preferred primary-combustor-outlet radial gas-temperature profile for turbine engines should be based on a compromise among combustor performance, allowable turbine blade temperature distribution, turbine aerodynamics, and the cooling requirements of the turbine casing and the stator outer and inner rings (hereinafter referred to as the turbine outer and inner shrouds). For uncooled turbines, the turbine blade stresses permit a temperature profile with the hottest region near the turbine blade tip where the stresses in the turbine rotor blades are low. Present turbo-jet combustors are designed to give this type profile, with maximum temperature variations between approximately 400° and 800° R. The preferred allowable turbine-inlet temperature profile for cooled turbines has not been investigated. Thus, it is important to know whether or not the gas-temperature profiles from present combustor designs are desirable or to what extent alterations might be profitable. Therefore, analyses were made at the NACA Lewis laboratory to evaluate the effects of turbine-inlet temperature (absolute total temperature at stator inlet) profile on the turbine rotor cooling-air requirements for shell-supported convection-cooled blades.

Shell-supported blades were chosen for this study because they are amenable to analytical treatment for determining cooling requirements. Similar studies could have been conducted for strut-supported air-cooled blades, but the analytical procedures are lengthy and use of an electrical analog is generally required. Also, at the present time no definite conclusions can be drawn concerning the relative superiority of shell-supported or strut-supported blades, and it appears that there will be fields of usefulness for each type of blade. It is believed, however, that the results obtained herein for shell-supported blades may be utilized in a general way to predict trends that would be obtained with strut-supported blades. For liquid-cooled blades, where the blade temperature is essentially equal to the liquid temperature, the blade temperature is almost constant, and the gas-temperature profile does not affect the coolant-flow requirements. Thus, a study of the effects of gas-temperature profile on the cooling-flow requirements for proposed liquid-cooled designs is generally unnecessary.

Turbine aerodynamic design has commonly been based on the assumption of uniform turbine-inlet temperature for both uncooled and cooled turbines. In addition, for cooled turbines the effective gas temperature (approximate total temperature relative to the turbine rotor) has been assumed to be uniform over the turbine blade span for analyses and design procedures for convection-cooled blades published in the literature (e.g., refs. 1 and 2). Although combustor-outlet profiles satisfying this condition can be obtained, it is at the expense of mixing pressure losses or combustor over-all length, or both. In general, the more nearly uniform the profile, the more difficult the combustor design problem becomes.

The gas-temperature profiles for efficient combustor design reported in the literature can be approximated with reasonable accuracy by a cosine wave (refs. 3 to 5). The profiles illustrated in reference 3 can be approximated by one-half cycle of the cosine wave with the hotter region near the turbine blade tip and the cooler region near the blade root. The profiles shown in reference 4 and some of those in reference 5 can be represented by a complete cycle of the cosine wave using a hot core with the cooler regions near both the blade root and the blade tip. With the complete cosine wave, the turbine inner and outer shrouds are exposed to the coolest gases and therefore require the minimum of cooling. In fact, for this design the average turbine-inlet temperature might be increased considerably without requiring shroud cooling. For the half cosine wave with the hotter gas layers near the blade tip region, the shroud cooling is minimized only on the inner shroud. However, the cooling load is translated to the outer shroud, which is more readily accessible.

The purpose of this report is to present the results of an analysis that compares the turbine rotor cooling requirements for the cosine-wave profiles with those for the uniform gas-temperature profile. In addition, the analysis is extended to determine the gas-temperature profile for the absolute minimum coolant flow. The absolute minimum coolant flow corresponds to an optimum gas-temperature profile. That is, for given turbine operating conditions, a minimum value of coolant flow can be obtained for gas-temperature profiles such as the uniform or cosine-wave profiles. For these same operating conditions, there is an optimum gas-temperature profile that gives a value of coolant flow smaller than those obtained for the other gas-temperature profiles. This value of coolant flow is the absolute minimum coolant flow. Turbine stator blade cooling is not considered. The low stresses imposed on the stator blades, however, permit freedom in the choice of stator blade designs not acceptable for the rotor blades.

The results are presented for average effective gas temperatures of 2500°, 3000°, and 3500° R and turbine blade design root stresses of 25,000 and 75,000 psi. For the effective gas-temperature profiles represented by cosine waves, a maximum variation in the gas-temperature profile of 800° R is used for most of the results. The effect of this variation on the coolant-flow requirements is also illustrated. Each blade design is defined by a cooling-effectiveness parameter, which is varied over a range sufficient to include all designs of practical interest.

3776

CE-1 back

ANALYTICAL PROCEDURES

Assumptions

Simplifying assumptions were necessarily introduced in this analysis in order to obtain convenient relations for the temperature distributions for convection-cooled turbine rotor blades. These assumptions have generally been used in the literature for computing the cooling-air requirements:

- (1) The effective gas temperature and the total gas temperature relative to the rotor blades are equal.
- (2) The radial heat conduction in the blade metal is negligible compared with the total heat transfer.
- (3) The outside and inside heat-transfer coefficients are constant over the blade outer and inner surfaces, respectively.
- (4) Radiation is negligible.
- (5) The effect of rotation on the cooling-air temperature rise is negligible.
- (6) The inner surface area upon which the inside effective heat-transfer coefficient is based is equal to the outer surface area. In addition, these areas are at the same temperature. (The effective heat-transfer coefficient is defined to include the heat conducting through auxiliary internal surfaces such as fins; this is defined in general terms in ref. 1.)
- (7) The chordwise blade temperature is constant.

For most cooled-turbine designs using air for convection cooling, calculations show that these assumptions, with the exception of assumption (5), have only slight effects on the cooling requirements. Reference 2 shows that, for high turbine blade tip speeds, the rotational effects on the cooling requirements may be large. However, for the present report, the rotational effects are neglected, since only a relative comparison of the cooling-air requirements for various gas-temperature profiles is made.

Basic Equations for Temperature Distributions

The change in the cooling-air temperature as it flows radially outward through the blade is given by the heat balance:

$$c_p w_a dT'_a = h_f l_1 (T_b - T'_a) dx \quad (1)$$

where all symbols are defined in appendix A. In addition, a balance between the heat transferred to the blade and that transferred to the coolant at any spanwise position gives the expression

$$h_o l_o (T_{g,e} - T_b) = h_f l_1 (T_b - T'_a)$$

or, with $l_o = l_1$,

$$\lambda (T_{g,e} - T_b) = T_b - T'_a \quad (2)$$

where $\lambda \equiv h_o/h_f$. The differential equation for the turbine blade spanwise temperature distribution is then obtained by solving equation (2) for T'_a and dT'_a/dx and substituting these expressions in equation (1). This equation can be reduced to

$$\frac{dT_{g,e}}{dx} + \frac{h_o l_o}{c_p w_a} \frac{1}{\lambda} T_{g,e} = \frac{1 + \lambda}{\lambda} \left(\frac{dT_b}{dx} + \frac{h_o l_o}{c_p w_a} \frac{1}{1 + \lambda} T_b \right)$$

It is convenient to nondimensionalize the spanwise position variable x by multiplying each term by the blade length b and rewriting the equation as

$$K \frac{dT_{g,e}}{dx^*} + \left(\frac{1 + \lambda}{\lambda} \right) T_{g,e} = \frac{1 + \lambda}{\lambda} \left(K \frac{dT_b}{dx^*} + T_b \right) \quad (3)$$

where

$$x^* \equiv \frac{x}{b} \quad (4)$$

and

$$K \equiv \frac{(1 + \lambda) c_p w_a}{h_o l_o b} \quad (5)$$

If the spanwise effective gas-temperature distribution is specified, equation (3) may be used to express the spanwise turbine blade temperature distribution as a function of the coolant-flow parameter K and the cooling-effectiveness parameter λ . The spanwise turbine blade temperature distribution must be limited by the maximum allowable turbine blade temperature distribution determined by the design stress and the stress-rupture characteristics of the material. Thus, the minimum allowable coolant-flow parameter for a specified effective gas-temperature distribution is obtained when the resulting blade temperature is equal to the allowable blade temperature at one spanwise location and equal to or less than the allowable temperature at all other locations.

If the spanwise turbine blade temperature distribution is specified, equation (3) may be used to express the spanwise effective gas-temperature distribution as a function of the coolant-flow parameter K and the cooling-effectiveness parameter λ . In this way the effective gas-temperature distribution for the absolute minimum value of the coolant flow for a given average effective gas temperature can be determined by specifying the most desirable turbine blade temperature distribution.

This report evaluates for given allowable blade temperature distributions both the absolute minimum value of the coolant-flow parameter and its corresponding effective gas-temperature distribution, and the minimum coolant-flow parameter for various given effective gas-temperature distributions. Thus, equation (3) is solved for both the effective gas-temperature distribution and the actual blade temperature distribution. In both cases, the allowable turbine blade temperature must be specified. Therefore, the allowable turbine blade temperature distributions as used in this report are first determined, after which equation (3) is solved for both the effective gas-temperature distribution and the blade temperature distribution. Then, the average effective gas temperature is determined. Finally, the effective gas temperature is related to the turbine-inlet temperature, which is of more importance in rating and analyzing the engine.

Allowable Spanwise Blade Temperature Distribution

The allowable turbine blade temperature is determined by the design value of the turbine blade stresses and the blade material stress-rupture properties. The allowable stress-rupture for any material depends on the life required as well as the temperature. In the present report, the stress-rupture properties are taken at 100-hour life.

The design value of the turbine blade stress is usually larger than the actual centrifugal stress for cooled turbine blades. This difference may be accounted for by introducing a constant of proportionality called the stress-ratio factor. The magnitude of the stress-ratio factor is meant to include the effects of other stresses, such as bending, vibration, and thermal stresses, as well as to provide some margin of safety for the effects that fabrication may have on the blade material strength (ref. 1). With gas-temperature profiles other than the uniform profile, the effects of thermal stresses may be intensified. Thus, the need for a stress-ratio factor becomes more apparent. As shown in reference 6, the design stress for a uniformly tapered turbine blade with a constant stress-ratio factor can be expressed by the equation

$$\sigma = S\rho U_t^2 f \left(\frac{A_{m,t}}{A_{m,h}}, \frac{r_h}{r_t}, x^* \right) \quad (6)$$

It is convenient to reduce the number of variables in equation (6) by expressing the root stress by equation (6) and then evaluating σ/σ_h . Thus,

$$\frac{\sigma}{\sigma_h} = F\left(\frac{A_{m,t}}{A_{m,h}}, \frac{r_h}{r_t}, x^*\right) \quad (7)$$

Equation (7) is plotted in figures 1(a) and (b) for three values of r_h/r_t and $A_{m,t}/A_{m,h}$. The ranges of r_h/r_t and $A_{m,t}/A_{m,h}$ were selected to include most values of practical interest according to present design procedures. This figure shows that r_h/r_t and $A_{m,t}/A_{m,h}$ have only secondary effects on the ratio of the stress at any spanwise position to that at the root, particularly, for the ranges in r_h/r_t encountered. Thus, representative values of r_h/r_t and $A_{m,t}/A_{m,h}$ may be selected to express σ/σ_h . This further reduces the number of design variables required in determining the allowable blade temperature distribution. For the present report, the stress equation (eq. (7)) is reduced to the simple expression

$$\frac{\sigma}{\sigma_h} = F(0.5, 0.65, x^*) = f(x^*) \quad (8)$$

corresponding to the mean curves in figures 1(a) and (b).

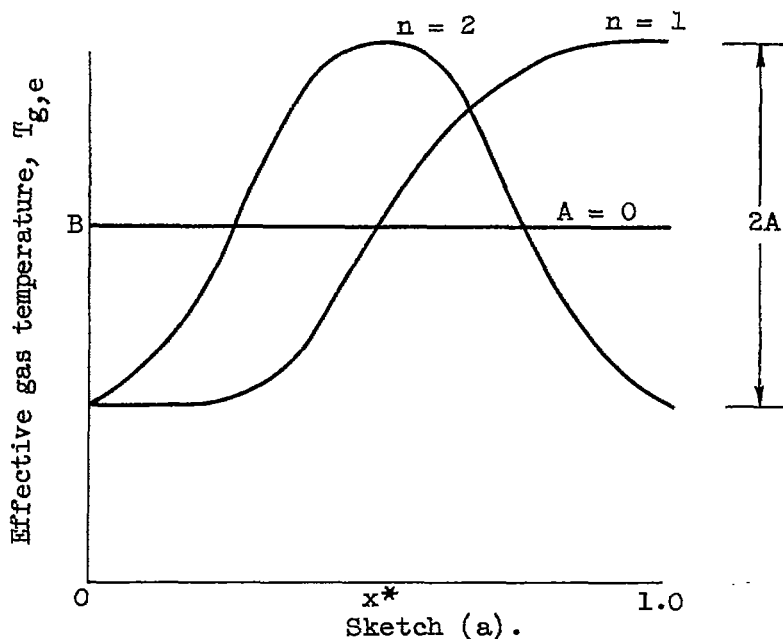
The allowable spanwise turbine blade temperature distribution can now be evaluated for any given design root stress by employing equation (8), once the stress-rupture properties are specified. The present report uses the 100-hour stress-rupture properties of a promising alloy with low critical metal content, A-286, for evaluating the allowable turbine blade temperature. The allowable spanwise turbine blade temperatures for A-286 with three turbine blade design root stresses are shown in figure 1(c). The extreme curves ($\sigma_h = 25,000$ and $75,000$ psi) give the allowable spanwise turbine blade temperatures used in the analyses of this report.

Minimum Coolant-Flow Parameter for Specified Effective Gas-Temperature Distribution

The effective gas-temperature distributions to be studied may be expressed by the equation

$$T_{g,e} = B - A \cos n\pi x^* \quad (9)$$

where the total variation in the effective gas temperature is given by $2A$. A sketch of the three profiles expressed by equation (9) is shown in sketch (a):



The following three cases are considered in this report:

(1) When $A = 0$, equation (9) represents the uniform profile.

(2) When A is a positive number and $n = 1$, it represents a profile with a hot layer near the turbine outer shroud and a colder layer near the turbine inner shroud.

(3) When A is a positive number and $n = 2$, it represents a profile with a hot core and colder layers near each turbine shroud.

For convenience, the equation is handled in the general form.

Equation (3) must now be solved for the effective gas-temperature distribution given by equation (9). The expression obtained when equation (9) is substituted into equation (3) is

$$\frac{dT_b}{dx^*} + \frac{1}{K} T_b = n\pi A \frac{\lambda}{1 + \lambda} \sin n\pi x^* + \frac{1}{K} (B - A \cos n\pi x^*) \quad (10)$$

This is a linear differential equation with the general solution

$$T_b = B + C_1 e^{-x^*/K} - \frac{A}{1 + (K n \pi)^2} \left\{ \frac{K n \pi}{1 + \lambda} \sin n\pi x^* + \left[\frac{(K n \pi)^2 \lambda}{1 + \lambda} + 1 \right] \cos n\pi x^* \right\} \quad (11)$$

The boundary condition for this equation is given by

$$T'_a = T'_{a,h}, \quad T_b = T_{b,h} \quad \text{at } x = 0 \quad (12)$$

For this position, equation (2) becomes

$$\lambda(B - A - T_{b,h}) = T_{b,h} - T'_{a,h} \quad (13)$$

But, from equation (11),

$$T_{b,h} = B + C_1 - A \left[\frac{(Kn\pi)^2 \lambda}{1 + \lambda} + 1 \right] \quad (14)$$

The constant of integration can be evaluated by eliminating $T_{b,h}$ from equations (13) and (14). The equation for the blade temperature distribution then becomes

$$T_b = B + \frac{e^{-x^*/K}}{1 + \lambda} (T'_{a,h} - B - \lambda A) - \frac{A}{1 + (Kn\pi)^2} \left\{ \frac{Kn\pi}{1 + \lambda} \sin n\pi x^* + \left[\frac{(Kn\pi)^2 \lambda}{1 + \lambda} + 1 \right] (\cos n\pi x^* - e^{-x^*/K}) \right\} \quad (15)$$

The minimum value of coolant-flow parameter K for each of the specified $T_{g,e}$ distributions can be evaluated for any cooling-air temperature $T'_{a,h}$ and allowable blade temperature distribution by use of equations (10) and (15). The solution is iterative. By writing equation (10) in the form

$$K = \frac{B - A \cos n\pi x^* - T_b}{\frac{dT_b}{dx^*} - n\pi A \frac{\lambda}{1 + \lambda} \sin n\pi x^*} \quad (16)$$

the minimum permissible value of K is obtained for the blade temperature T_b equal to the allowable blade temperature at the specified spanwise position x^* . At all other locations, the blade temperature must be equal to or less than the allowable temperature. Equation (15) can be written

$$T'_{a,h} = B + \lambda A - (1 + \lambda) e^{x^*/K} x \left(B - T_b - \frac{A}{1 + (Kn\pi)^2} \left[\frac{Kn\pi}{1 + \lambda} \sin n\pi x^* + \frac{[(Kn\pi)^2 \lambda + 1]}{1 + \lambda} (\cos n\pi x^* - e^{-x^*/K}) \right] \right) \quad (17)$$

Substitution of K from equation (16) into equation (17) provides the value of cooling-air temperature at the blade root $T'_{a,h}$ for the conditions specified. Choice of a different value of x^* in equation (16) will result in different values of K and $T'_{a,h}$. In this manner, the minimum permissible value of coolant-flow parameter can be evaluated for a range of cooling-air temperatures by assuming a cooling-effectiveness parameter λ , an allowable turbine blade temperature distribution as determined from stress calculations, and a range of values of x^* where the blade temperature will equal the allowable blade temperature.

This procedure is employed in this report considering the three effective gas-temperature profiles prescribed earlier: (1) uniform profile with $A = 0$, (2) half-cosine-wave profile with A finite and $n = 1$, and (3) complete-cosine-wave profile with A finite and $n = 2$. In each case three values of B (2500° , 3000° , 3500° R) are specified.

Absolute Minimum Coolant-Flow Parameter and Corresponding Effective Gas-Temperature Distribution

If the spanwise blade temperature distribution requiring an absolute minimum coolant flow is known, equation (3) can be solved to determine the corresponding effective gas-temperature distribution (hereinafter referred to as the optimum effective gas-temperature profile). Since equation (3) is a first-order linear differential equation, the general solution can be expressed as

$$T_{g,e} = e^{-\left(\frac{1+\lambda}{\lambda} \frac{x^*}{K}\right)} \left[\frac{1+\lambda}{\lambda} \int_0^{x^*} \left(\frac{dT_b}{dx^*} + \frac{T_b}{K} \right) e^{\left(\frac{1+\lambda}{\lambda} \frac{x^*}{K}\right)} dx^* + C_2 \right] \quad (18)$$

Introducing the boundary condition as given by equation (12), the constant of integration can be evaluated in a manner similar to that of the last section. The equation becomes

$$T_{g,e} = e^{-\left(\frac{1+\lambda}{\lambda} \frac{x^*}{K}\right)} \left[\frac{1+\lambda}{\lambda} \int_0^{x^*} \left(\frac{dT_b}{dx^*} + \frac{T_b}{K} \right) e^{\left(\frac{1+\lambda}{\lambda} \frac{x^*}{K}\right)} dx^* + \frac{T_{b,h}(1+\lambda) - T'_{a,h}}{\lambda} \right] \quad (19)$$

The integral in equation (19) can be integrated once by parts to further reduce the equation to

$$T_{g,e} = \frac{1+\lambda}{\lambda} T_b - e^{-\left(\frac{1+\lambda}{\lambda} \frac{x^*}{K}\right)} \left(\frac{1+\lambda}{K\lambda^2} \int_0^{x^*} T_b e^{\left(\frac{1+\lambda}{\lambda} \frac{x^*}{K}\right)} dx^* + \frac{T'_{a,h}}{\lambda} \right) \quad (20)$$

Equation (20) has been used to determine the optimum effective gas-temperature profile and the corresponding absolute minimum coolant-flow parameter. Appendix B shows that the spanwise blade temperature distribution satisfying this condition is the allowable temperature distribution. Since the allowable blade temperature distribution cannot be explicitly expressed, equation (20) is solved numerically. The integral is evaluated using Simpson's rule of replacing the integrand by parabolas. In this way, the blade span is divided into ten equal segments. The procedure employed is to assume several values of the coolant-flow parameter K for each combination of cooling-effectiveness parameter λ , cooling-air temperature $T'_{a,h}$, and allowable turbine blade temperature distribution.

Basis for Comparison of Results

The comparison of the cooling requirements for each effective gas-temperature profile was made by computing the ratio of the coolant weight flow for either the optimum temperature profile or the temperature profiles representable by the cosine or half-cosine waves to that for the uniform temperature profile. The uniform temperature profile is used as the reference, since it is the basis for all cooling results and procedures published in the literature. All comparisons are made for the same values of average effective gas temperature $\bar{T}_{g,e}$, blade design root stress σ_h , cooling-air temperature $T'_{a,h}$, and blade geometry. Values of $T'_{a,h}$ and σ_h are independently assigned. The procedures for evaluating $\bar{T}_{g,e}$ and the coolant-flow ratio so that the blade geometry is maintained constant are given in the following sections. In order to obtain even values of $\bar{T}_{g,e}$ (i.e., 2500°, 3000°, and 3500° R), it is necessary to interpolate the coolant-flow results obtained for the optimum and half-cosine-wave gas-temperature profiles.

Calculation of average effective gas temperature. - The average effective gas temperature $\bar{T}_{g,e}$ is defined as

$$\bar{T}_{g,e} w_g = \int_{r_h}^{r_t} T_{g,e} \rho_g V_{x,g} 2\pi r dr \quad (21)$$

or, expressing the total gas flow w_g in the integral form, equation (21) becomes

$$\bar{T}_{g,e} = \frac{\int_{r_h}^{r_t} T_{g,e} \left(\frac{\rho_g V_{x,g}}{\rho_g^* a_{cr}} \right) r \, dr}{\int_{r_h}^{r_t} \left(\frac{\rho_g V_{x,g}}{\rho_g^* a_{cr}} \right) r \, dr} \quad (22)$$

In this definition, the average effective gas temperature is a measure of the total energy of the gas relative to the turbine rotor. For free-vortex turbine designs the specific-mass-flow parameter $\rho_g V_{x,g} / \rho_g^* a_{cr}$ can be approximated as a linear function of the spanwise position. (A linear function is convenient to facilitate the integration in equation (22).) To obtain this functional relation, it is necessary to specify the value of $\rho_g V_{x,g} / \rho_g^* a_{cr}$ at a given spanwise position. For this analysis the value of $\rho_g V_{x,g} / \rho_g^* a_{cr}$ is specified at the turbine rotor blade hub to correspond to a turbine design having a flow angle of 25° and an absolute Mach number of 1.0 at the stator exit, resulting in the following equation:

$$\frac{\rho_g V_{x,g}}{\rho_g^* a_{cr}} = 0.2679 + 0.0684x^* \quad (23)$$

The values of flow angle and Mach number used to obtain equation (23) are considered typical for present turbine designs. However, the final cooling results would be only slightly affected if the values of the flow angle and Mach number were considerably different from those chosen.

Equations (22) and (23) are used to obtain $\bar{T}_{g,e}$ for each effective gas-temperature distribution. For the uniform profile and the profile given by the complete cosine wave ($n = 2$), the integration of equation (22) results in $\bar{T}_{g,e} = B$ (see eq. (9)). For the half-cycle cosine-wave profile, integration of equation (22) results in the expression

$$\bar{T}_{g,e} = B + 0.1308A$$

Finally, for the optimum profile the integration of equation (22) must be carried out numerically for each effective gas-temperature profile.

Calculation of coolant-flow ratios. - The ratio of the coolant weight flow obtained for the optimum or cosine-wave gas-temperature profiles to that for the uniform profile is computed from equation (5) with the expression

$$\frac{w_a}{w_{a,un}} = \frac{K}{K_{un}} \left(\frac{1 + \lambda_{un}}{1 + \lambda} \right) = \frac{K}{K_{un}} \left[\frac{1 + \lambda_{un}}{1 + \lambda_{un} \left(\frac{\lambda}{\lambda_{un}} \right)} \right] \quad (24)$$

recognizing that all other terms in equation (5) may be held constant for a particular design.

It is further desirable to make a comparison such that the blade geometries are the same. For this condition, it may not be assumed that λ is unchanged, since for turbulent flow λ depends on the coolant flow. Thus, for particular engine design conditions and a given blade design,

$$\frac{\lambda}{\lambda_{un}} = \frac{h_{f,un}}{h_f} \approx \frac{h_{i,un}}{h_i} = \left(\frac{w_{a,un}}{w_a} \right)^c \quad (25)$$

The approximation given in equation (25) results from the relative change in the thermal gradients in any auxiliary heat-transfer surfaces due to the change in coolant flow. For the coolant-flow changes of interest, this approximation may be assumed to be valid. Substituting equation (25) into equation (24) gives

$$\frac{w_a}{w_{a,un}} = \frac{K}{K_{un}} \left[\frac{1 + \lambda_{un}}{1 + \lambda_{un} \left(\frac{w_{a,un}}{w_a} \right)^c} \right] \quad (26)$$

where the exponent c is zero for laminar flow and 0.8 for turbulent flow (see ref. 2). It must be recalled that K itself depends upon the particular value of λ assigned. Therefore, in obtaining $w_a/w_{a,un}$ from equation (26) for a given λ_{un} , it is necessary to use the value of K corresponding to the value of λ given by equation (25). Thus, an iterative solution is used to calculate the coolant-flow ratios in this report. This is done by first assuming that $\lambda = \lambda_{un}$ and then solving equation (26) for $w_a/w_{a,un}$. Then, with this value of $w_a/w_{a,un}$, λ/λ_{un} is computed from equation (25) and, thus, from its definition, a corrected value of K .

Relation Between Effective Gas and Turbine-Inlet Temperatures

Since engines are rated and analyzed on the basis of the turbine-inlet temperature, it is desirable to relate the effective gas-temperature relative to the turbine rotor, as used in the preceding sections, to the turbine-inlet temperature. In order to obtain a simple relation with relatively few variables so that the results could be easily interpreted, the following simplifying assumptions are made:

- (1) The turbine is of free-vortex design.
- (2) Impulse conditions exist at the turbine hub section.
- (3) No turbine-exit whirl exists.
- (4) The turbine efficiency is 1.00.
- (5) The effective and total gas temperatures relative to the turbine are the same.

Although the first three assumptions are reasonable for present gas-turbine design practices, the latter two may result in slight errors in the temperature differences. However, calculations show that the computed temperature differences are, in all cases, within approximately 50° of the actual values. This is considered acceptable in the present analysis particularly, in view of the simplicity afforded.

The relations for the difference between the total turbine-inlet temperature and the effective gas temperature are derived in appendix C. This difference at any spanwise position is given by the equation

$$T_1' - T_{g,e} = \frac{\gamma-1}{2\gamma gR} U_t^2 \left(\frac{r_h}{r_t}\right)^2 \left\{ 4 - \left[1 + x^* \left(\frac{r_t}{r_h} - 1\right) \right]^2 \right\} \quad (27)$$

The integration of equation (27) to obtain the difference between the average of these temperatures gives

$$\bar{T}_1' - \bar{T}_{g,e} = \frac{\gamma-1}{4\gamma gR} U_t^2 \left(\frac{r_h}{r_t}\right)^2 \left[7 - \left(\frac{r_t}{r_h}\right)^2 \right] \quad (28)$$

Equations (27) and (28) are plotted in figures 2(a) and (b), respectively, for $\gamma = 4/3$ considering two turbine hub-tip radius ratios. Figure 2(a) illustrates the distortion of the effective gas-temperature distributions required to obtain the total turbine-inlet temperature. Figure 2(b) illustrates the average change. Both the distortion and the average change may be useful in converting the prescribed and computed effective gas-temperature distributions into the more familiar turbine-inlet temperature.

RANGES OF INDEPENDENT VARIABLES

The coolant-flow parameter K may be evaluated for any desired average effective gas temperature $\bar{T}_{g,e}$ and a given effective gas-temperature profile with the procedures previously outlined. The value of K also depends on the choice of the cooling-effectiveness parameter

λ , turbine blade design root stress σ_h , and blade-inlet cooling-air temperature $T'_{a,h}$. Thus, in order to make this study as general as possible, it is necessary to choose ranges of the independent variables so that all cooled-turbine designs of interest are included. The ranges of independent variables chosen for this analysis are as follows; the reasons for the choices are discussed in subsequent sections:

| | |
|--|-------------------|
| Cooling-effectiveness parameter, λ_{un} | 0.15, 0.30, 0.65 |
| Blade design root stress, σ_h , psi | 25,000 and 75,000 |
| Blade-inlet cooling-air temperature, $T'_{a,h}$, $^{\circ}R$ | 600, 1000, 1300 |
| Average effective gas temperature, $\bar{T}_{g,e}$, $^{\circ}R$ | 2500, 3000, 3500 |

Cooling-Effectiveness Parameter

The values of the cooling-effectiveness parameter λ_{un} selected for this study were chosen from experience acquired with the corrugated-insert blade for both single-stage and two-stage turbines. The value of λ_{un} is inversely related to the amount of internal surface area within the coolant passage and the actual inside heat-transfer coefficient. These two effects combine in such a way that the minimum value of λ_{un} is limited by either the blade size (in this case the area increases so that the blade size becomes unacceptable), the pressure drop, or the mass-flow capacity. Any number of blade designs corresponding to different values of λ_{un} may be selected for cooling a specific engine design. Examples of this are the various blade designs presented in reference 7 for each engine design. Experience shows that design values of λ_{un} near 0.30 seem most reasonable for existing convection-cooled blade designs. Values of λ_{un} near 0.65 or greater may be suitable for many engine design conditions requiring little cooling. However, in such cases, the design value of λ_{un} can be lowered without disadvantage. Values of λ_{un} below 0.30 can and have been obtained. However, values of λ_{un} near 0.15 as used for the lower limit of this report represent extremely effective blade designs that have not been encountered. Probably such values are reasonable only for improved blade designs or designs using a more effective coolant than air (e.g., this approaches the condition for liquid-cooled designs).

Blade Design Root Stress

At present, uncooled turbines are designed for blade design root stresses σ_n of around 25,000 psi. However, in many cases, the trend is to increase the blade stresses by decreasing hub-tip radius ratio in the interest of increasing both the compressor and turbine work per stage and the weight-flow capacity. Experience also shows that cooled turbines

must presently be designed for blade root stresses higher than those indicated by the centrifugal load to account for other stresses, as discussed in a preceding section. For these reasons, a high blade root design stress of 75,000 psi was also considered.

Blade-Inlet Cooling-Air Temperature

Values of blade-inlet cooling-air temperature can be inferred from figure 3, where the cooling-air bleed temperature is plotted against the cooling-air bleed pressure ratio. The bleed point referred to in figure 3 may be at the compressor exit or at some intermediate stage of the compressor. (Ref. 7 discusses in detail the effects of compressor bleed point on rotor blade coolant flows.) A typical operating line presently anticipated for turbojet engines designed for supersonic flight up to Mach number of 2.5 is illustrated in figure 3 for equal cooling-air bleed pressure ratio and compressor pressure ratio. For the case shown, the take-off compressor pressure ratio is 10, and it is assumed that the engine operates at constant mechanical speed. The range in compressor-discharge temperatures illustrated by the operating line in figure 3 varies between a lower limit of around 1000° R and an upper limit of around 1400° R. Although this lower limit is acceptable for turbine cooling, experience shows that cooling-air temperatures of 1400° R are probably excessive, and bleed ahead of the compressor discharge or else cooling of the bleed air will be required. Reference 7 indicates that, for a flight Mach number of 2.0 with single-stage turbines driving compressors having pressure ratios near the typical values shown in figure 3, the cooling-air temperature may be reduced by about 200° R by bleeding ahead of compressor discharge. Calculations obtained for two-stage turbine designs at the same conditions indicate similar results. Thus, at a flight Mach number of 2, the cooling-air temperatures, as suggested by available calculations, are about 1000° R and above for compressor pressure ratios anticipated. Since low-pressure-ratio subsonic engine designs (such designs are in present application) require cooling-air temperatures somewhat below 1000° R, and engines operating at Mach numbers around 2.5 may have temperatures near 1400° R, a cooling-air temperature range from 600° to 1300° R was chosen for this study.

Average Effective Gas Temperature

Since the analytical procedures employed in this analysis permit an arbitrary choice of the average effective gas temperature $\bar{T}_{g,e}$, values of 2500°, 3000°, and 3500° R were chosen for convenience in calculations. This range of values should adequately cover the cooled-turbojet-engine designs anticipated.

RESULTS AND DISCUSSION

3776

The average effective gas temperature is used throughout as an independent variable in comparing the various effective gas-temperature profiles considered, because it is convenient and reduces the variables involved. Since engines are rated by the turbine-inlet temperature, the conversion to turbine-inlet temperature is required. Figure 2 shows that this conversion results in an average turbine-inlet temperature higher than the average effective gas temperature. In addition, the turbine-inlet temperature profile relative to the effective gas-temperature profile is distorted by increasing the differential at the root more than at the tip. This tends to increase the root total temperature relative to the tip total temperature. For a turbine hub-tip radius ratio between 0.60 and 0.75 and a tip speed of 1100 feet per second, the distortion as given by figure 2(a) is between 60° and 40° R from root to tip. For this case, the average total temperature varies between approximately 70° and 135° R above the average effective gas temperature (see fig. 2(b)). Thus, for an average effective gas temperature of 2500° R and a hub-tip radius ratio near 0.70, the average turbine-inlet temperature is about 2600° R. These design conditions are typical for current design practice. Thus, the correction from effective to turbine-inlet temperatures, as stated previously, may be used as a reasonable correction to be applied throughout the present report. An increase in the tip speed above 1100 feet per second results in an increase in the turbine-inlet temperature for a given effective gas temperature. Similarly, the distortion of the total gas-temperature profile with respect to the effective gas-temperature profile increases as the tip speed increases. This spanwise distortion increases by the same percentage as the difference between the average total and effective gas temperatures.

Illustrative Spanwise Temperature Distributions

The spanwise variations in the corresponding effective gas temperature, allowable blade temperature, and actual blade temperature are illustrated in figure 4 for each effective gas-temperature profile considered. The conditions for these distributions are representative of those desirable for high-temperature engine designs of immediate interest: $\bar{T}_{g,e} = 2500^\circ \text{R}$, $\bar{T}_l \approx 2600^\circ \text{R}$, $\lambda = 0.30$, $\sigma_h = 25,000 \text{ psi}$, and $T_{a,h}^* = 1000^\circ \text{R}$. For the effective gas-temperature profiles representable by the cosine wave, the maximum variation in effective gas temperature is 800° R (cosine-wave amplitude A of 400° R). For the conditions of figure 4, the blade is overcooled near the root for all effective gas-temperature profiles except the optimum profile. In the regions where the blade is overcooled, the effective gas temperature may be increased for a given coolant flow to permit the actual blade temperature to reach the allowable value. If the actual blade temperature equals the allowable value, the absolute

minimum coolant flow is obtained, and the resulting effective gas-temperature profile is the optimum profile. Such a profile is illustrated in figure 4(d). In this case, the effective gas temperature at the blade root is extremely high. This results in a large heat-transfer rate, which rapidly increases the cooling-air temperature from root to tip, and, thus, in turn the effective gas temperature decreases. The lowest effective gas temperature then occurs in the region of the turbine blade midspan.

The effective gas temperature for the absolute minimum coolant flow as shown in figure 4(d) exceeds stoichiometric at the blade root and, therefore, cannot be obtained with hydrocarbon fuels. Probably, in this case, the temperature could be lowered within this limit and still approximate conditions for the absolute minimum coolant flow. If the maximum temperature is limited to stoichiometric temperature, these optimum profiles are acceptable for combustor designs and are probably easier to obtain than the uniform profile. However, these profiles present acute inner-shroud cooling problems.

As the conditions for cooling become more critical or as the blade cooling effectiveness decreases (λ increases), the coolant-flow requirements increase. As the coolant flows increase, the actual blade temperature becomes less sensitive to the heat transfer. This results in less overcooling near the root regions for the uniform temperature profile and the two temperature profiles representable by the cosine wave. In fact, for the uniform temperature profile, the critical point where the actual and the allowable blade temperatures are equal may occur at the root. Since the overcooling has been reduced, the effective gas-temperature profile becomes more favorable for the shroud. Figure 5 illustrates the effect on optimum effective gas-temperature profiles of making the cooling conditions more critical or of reducing the blade cooling effectiveness. For convenience, the value of $\bar{T}_{g,e}$ used in figure 5 is an integrated average rather than a mass average as given by equation (22). Use of an integrated average in these instances had a negligible effect on the trends and quantitative values shown in figure 5. An inspection of these results quickly shows that the gradients in the optimum effective gas-temperature profile decrease with increasing values of the average effective gas temperature, blade design root stress, cooling-air temperature at the blade root, or cooling-effectiveness parameter. In all cases the optimum effective gas temperature results in critical conditions for inner-shroud cooling. It is also apparent that the best conditions exist for a high value of the cooling-effectiveness parameter. However, this, in general, corresponds to a poor blade design that requires high coolant flows and is inadequate for cooling in many cases.

Comparison of Cooling Requirements for Each Effective
Gas-Temperature Profile

3776

The ratio of coolant flow for each effective gas-temperature profile to that for the uniform profile is plotted against the blade-inlet cooling-air temperature in figure 6. The effects of cooling-effectiveness parameter λ_{un} , blade design root stress σ_h , and average effective gas temperature $\bar{T}_{g,e}$ are shown in these plots. For these figures, the maximum variation in the effective gas temperatures representable by a cosine wave is 800°R ($A = 400^\circ\text{R}$). For a $\bar{T}_{g,e}$ of 3000°R , the cooling-air weight-flow ratio $w_a/w_{a,un}$ was obtained only for the optimum effective gas-temperature profile except for $\lambda_{un} = 0.30$. As pointed out previously, a value of λ_{un} near 0.30 is reasonable for existing convection-cooled blade designs. The cross-hatched region for each effective gas-temperature profile represents the complete range from turbulent to laminar flow for the cooling air. The curve terminating the cross-hatched area nearest values of $w_a/w_{a,un}$ of unity represents turbulent flow, while the other terminal curve represents laminar flow. For cooled engines employing convection-cooled blades, the cooling-air flow is either in the laminar region or in the transition region near the laminar flow limit (ref. 7). Turbulent flow would be expected to occur for low-altitude flight at high flight speeds, a combination not often considered. Therefore, the laminar lines on these figures are presently more applicable. In many cases, however, the effect of the flow region is small.

Cooling-effectiveness parameter of 0.15. - For an effective cooled-blade design ($\lambda_{un} = 0.15$), solutions were obtained for all the conditions considered in this analysis (fig. 6(a)). As the blade-inlet cooling-air temperature increases, the coolant-flow ratio for the various profiles is essentially unaffected except for $\sigma_h = 75,000$ psi, $\bar{T}_{g,e} = 3500^\circ\text{R}$, and the complete-cosine-wave profile. At the low-stress condition ($\sigma_h = 25,000$ psi), the effective gas-temperature profile represented by the complete cosine wave is, in general, better than that represented by the half-cycle cosine wave. For both the complete and the half-cycle cosine waves, the required coolant-flow ratios are near that for the uniform profile. At the high stress condition ($\sigma_h = 75,000$ psi), the profile represented by the half-cycle cosine wave becomes better than that represented by the complete cosine wave. It is of interest to note that, as the coolant-flow ratio for the temperature profile represented by the complete cosine wave becomes higher, that represented by the half-cycle wave tends to become better. In all cases, the optimum effective gas-temperature profile shows gains in coolant-flow ratio over the other profiles, being approximately 10 percent below the coolant flow obtained with the uniform profile.

Cooling-effectiveness parameter of 0.30. - Increasing the value of λ_{un} to 0.30 (decreasing blade cooling effectiveness) decreases the number of solutions (fig. 6(b)), and the effect of the gas-temperature profiles on the coolant-flow ratio $w_a/w_{a,un}$ becomes more apparent. At the high stress and high average effective gas temperature, the lack of completeness of the curves indicates that no solutions were obtainable. The same trends observed for $\lambda_{un} = 0.15$ are true for $\lambda_{un} = 0.30$, except that the coolant-flow rates are in general higher than those obtained for $\lambda_{un} = 0.15$.

Cooling-effectiveness parameter of 0.65. - A further increase in λ_{un} to 0.65 (further decreasing the blade cooling effectiveness) again decreases the number of solutions and increases the effects of gas-temperature profile on the coolant-flow ratio (fig. 6(c)). For this case, the only possible solutions at the two highest average effective gas temperatures exist for the low blade-inlet cooling-air temperatures. At $\bar{T}_{g,e}$ of 2500° R, solutions were obtained over the complete range of blade-inlet cooling-air temperatures at σ_h of 25,000 psi. In general, the cosine profiles require high relative coolant flows. These results suggest that care must be extended when subjecting blades having poor cooling effectiveness to the effective gas-temperature profiles represented by cosine waves if these blades are designed and analyzed for uniform gas-temperature profiles. The advantage of the optimum gas-temperature profile in reducing the coolant-flow requirements decreases as the blade-inlet cooling-air temperature or blade root design stress increases.

Evaluation of Effective Gas-Temperature Profiles for Cooled-Engine Designs of Immediate Interest

It has been mentioned that cooled-engine design conditions of immediate interest correspond to turbine blade design root stresses of about 25,000 psi, average effective gas temperatures of 2500° R (average turbine-inlet temperature near 2600° R), and a cooling-effectiveness parameter of 0.30. Also, for the same values of $\bar{T}_{g,e} = 2500^\circ$ R and $\lambda_{un} = 0.30$, it is of interest to evaluate the effective gas-temperature profiles at the higher blade root stress ($\sigma_h = 75,000$ psi). As previously discussed, higher stresses may be necessary for cooled-engine designs. Consequently, the effects of the various effective gas-temperature profiles on the coolant-flow requirements for engines having $\bar{T}_{g,e}$ of 2500° R and λ_{un} of 0.30 for σ_h of 25,000 and 75,000 psi are briefly discussed.

5776

Blade design root stress of 25,000 psi. - For the optimum effective gas-temperature distribution and the engine design conditions just described, the rotor blade coolant flow is about 20 percent below that of the uniform gas-temperature profile for blade-inlet cooling-air temperatures (1000° to 1300° R) encountered for flight Mach numbers around 2.0 to 2.5 (fig. 6(b)(1)). It is informative to reflect this reduction in coolant flow into potential improvements in the engine performance. According to the results of reference 7, the actual turbine rotor blade coolant flow for these engine design conditions would probably not exceed 4 percent of the compressor weight flow. Reference 8 indicates that a 20-percent saving in this coolant flow would not have much effect on the specific fuel consumption of the turbojet engine and only a small effect on the turboprop engine but would increase the thrust and horsepower of these engines by about 1 percent. This represents the probable maximum potential for these design conditions. Even if the need for inner-shroud cooling (due to the optimum temperature profile) does not offset this advantage, it seems likely that the mechanical complexity will. For higher turbine-inlet temperatures and correspondingly higher coolant weight flows, the improvements might be more pronounced, particularly if the optimum gas-temperature profile is maintained through several cooled stages. Thus, despite the problems such as inner-shroud cooling that are associated with the optimum profile, the improvements in engine performance derived from turbine cooling might be sufficiently great to warrant the use of this profile.

For a flight Mach number of 2.0, the blade-inlet cooling-air temperature may be about 1000° R if the cooling air is bled ahead of the compressor discharge. At this cooling-air temperature and the engine design conditions of $\bar{T}_{g,e}$ of 2500° R and λ_{un} of 0.30, the coolant weight flow for the gas-temperature profile represented by the complete cosine wave is about 7 percent higher than that for the uniform profile. Increasing the flight Mach number results in an increase in blade-inlet cooling-air temperature and a further increase in the coolant flow for the complete-cosine-wave profile compared with that of the uniform profile (fig. 6(b)). At a blade-inlet cooling-air temperature of 1300° R, a value anticipated for a flight Mach number around 2.5, the coolant flow for the complete cosine wave is about 35 percent higher than that for the uniform profile. This increase would probably be reflected into approximately a 1- and 2-percent loss in thrust and horsepower, respectively, for the turbojet and turboprop engines. Also, for the engine design conditions being considered, the gas-temperature profile represented by the half-cycle cosine wave results in no advantage over that for the complete cosine wave. Thus, for engine designs having σ_h of 25,000 psi, $\bar{T}_{g,e}$ of 2500° R, and λ_{un} of 0.30, the effective gas-temperature profile given by the complete cosine wave is comparable for turbine blade cooling to the uniform profile for blade-inlet cooling-air temperatures up to 1000° R (or flight Mach numbers up to around 2.0). In addition, this

profile permits combustor design simplification with a minimum of shroud cooling without sacrificing cooling-air flow. At blade-inlet cooling-air temperatures above 1000° R, the blade cooling effectiveness may be increased (λ_{un} decreased) in order to apply the complete-cosine-wave profile without significant losses in engine performance.

Blade design root stress of 75,000 psi. - In the future, turbine and compressor designs may be improved by increasing the blade root stresses. For turbine blade design root stresses in the neighborhood of 75,000 psi, the cooling-air requirement for the effective gas-temperature profile represented by the half cycle of the cosine wave is, in general, better than that represented by the complete cycle (fig. 6(b)). In addition, the cooling requirements for this profile compare favorably with the uniform profile (within about 10 percent). Thus, in general, little sacrifice in engine performance is required if a half-cycle cosine-wave gas-temperature profile is employed. For values of $\lambda_{un} = 0.30$, it appears that the profile given by the complete cosine wave would not be desirable for high-stress engine designs unless $T_{a,h}^*$ is below 1000° R and $\bar{T}_{g,e}$ is below 3000° R. This situation is improved to some extent by improving the blade cooling effectiveness and thereby reducing λ_{un} as shown by figure 6(a).

Effect of Combustor Pressure Losses on Engine Performance

The disadvantage of the uniform effective gas-temperature profile resulting from the additional pressure drop required in the combustor cannot be immediately evaluated, because the pressure losses required can only be inferred from the literature. However, it can be easily shown from the engine cycle analysis that large combustor pressure losses must be sustained in order to cause large engine thrust losses, particularly at high flight Mach numbers. This fact is illustrated by figure 7, where the ratio of the turbojet thrust for prescribed combustor pressure losses to the thrust for no combustor pressure loss is plotted against the flight Mach number for three combustor total-pressure ratios. The ordinate of figure 7 is inversely proportional to the increase in the specific fuel consumption required. As the combustor total-pressure ratio is decreased from 1 to 0.9, the maximum decrease in the thrust is 4 percent. At the higher flight Mach numbers, the decrease in thrust accompanying this decrease in the combustor pressure ratio is only about 3 percent. Thus, the thrust change is about one-third of the change in the total combustor pressure ratio. A similar trend occurs in reducing the combustor pressure ratio from 0.9 to 0.8. It is therefore apparent that the use of the uniform effective gas-temperature profile would not result in large increases in specific fuel consumption due to combustor pressure losses. It must be remembered, however, that the uniform profile may result in severe turbine shroud cooling problems.

Effect of Maximum Temperature Variation of Cosine-Wave Profiles
on Cooling Requirements

3776 The ratios of the cooling-air weight flow for the effective gas-temperature profiles representable by the complete and half-cycle cosine waves and that for the uniform gas-temperature profile are plotted in figure 8 for several values of the cosine amplitude A . It may be recalled that for $A = 0$ the effective gas-temperature profile is uniform. This is the limiting case for the results in figure 8 and corresponds to the value $w_a/w_{a,un} = 1$. Figure 8 is limited to an average effective gas temperature of 2500° R and laminar flow for the cooling air as well as $\lambda_{un} = 0.30$, since these design conditions seem feasible for the near future. For present combustor designs that exhibit good performance, the maximum variation of the effective gas temperature is approximately from 400° to 800° R (A of 200° to 400° R). Figure 8 illustrates that, as A increases, the cooling requirements, in general, increase continually at about the same rate. For most design conditions of interest, the maximum variation of 800° to 1200° R (A of 400° to 600° R) increases the coolant-flow ratio by only about 10 percent. Of course, correspondingly, an equal decrease in the maximum temperature variation results in a reduction of the coolant flow of the order of 10 percent. It is impractical at present to attempt to evaluate these changes in detail. However, according to the performance changes previously quoted, the effect of these coolant-flow changes on the performance is small.

CONCLUDING REMARKS

Each engine and convection-cooled blade design presents a unique problem, which in most cases fits somewhere within the framework of the results of this report. In some cases it may be desirable to obtain a detailed comparison of the advantages or disadvantages of one or more gas-temperature profiles. Such detailed studies might be of particular interest for those design conditions for which the coolant flow is affected appreciably by the gas-temperature profile. These detailed studies would involve an evaluation of combustor performance as well as calculations of turbine shroud-cooling requirements. In addition, consideration should be given to the effects of the gas-temperature profile on the turbine aerodynamics. In fact, in no case can any particular profile be completely justifiable until the turbine aerodynamics is studied. Where a detailed study is desirable, it is suggested that the turbine rotor cooling analysis be completed using the established procedures for a uniform effective gas-temperature profile. The results of this report can then be used to reflect the computed cooling requirements into those for the other effective gas-temperature profiles. However, in many cases, engineering judgment based on the general results of this report is sufficient for selecting the gas-temperature profile for a specific design. These general results may be summarized as follows:

1. The cooling-air flow required for blade designs with poor cooling effectiveness or for severe cooling conditions may be considerably higher for the effective gas-temperature profiles represented by the cosine waves (approximating present high-performance combustor designs) than for the uniform profile. This suggests that care must be extended in applying a blade designed for a uniform effective gas-temperature profile to the gas-temperature profile represented by the cosine waves. This difficulty with the poorly cooled blade designs can probably be eliminated in most cases of present interest by improving the blade cooling effectiveness (decreasing cooling-effectiveness parameter).

2. For design conditions of most immediate interest (design compressor pressure ratio of 10, design root stress near 25,000 psi, turbine-inlet temperatures around 2600° R, and blade designs having a cooling-effectiveness parameter near 0.30), the effective gas-temperature profile represented by the complete cycle of the cosine wave with a maximum variation of 800° R requires about 7 percent more cooling air than that for the uniform profile except for a blade-inlet cooling-air temperature above 1000° R (flight Mach number around 2.0). For a Mach number near 2.5, the cooling-air flow for this condition might be increased by about 35 percent. This increase would probably be reflected into approximately a 1- and 2-percent loss in thrust and horsepower, respectively, for the turbojet and turboprop engines. However, with this complete-cosine-wave profile, the turbine inner and outer shrouds are exposed to the lowest gas temperature and may, therefore, require either no cooling or at least a minimum of cooling while good combustor performance is afforded.

3. As the design blade stress is increased, the effective gas-temperature profile given by the complete cycle of the cosine wave becomes less favorable, but the profile represented by one-half cycle of the cosine wave becomes more favorable. For a high design stress of 75,000 psi, blade cooling-effectiveness parameter of 0.30, and turbine-inlet temperature of 2600° R, this half-cycle cosine profile requires about 10 percent more cooling air than the uniform profile for flight Mach numbers up to about 2.0. This increase diminishes to nearly zero at a flight Mach number of 2.5. Thus, for these conditions, the engine performance would be affected only slightly. On the other hand, with the gas-temperature profile represented by this one-half cycle of the cosine wave, the inner-shroud cooling problem is minimized at the expense of additional cooling on the more accessible outer shroud.

4. The optimum effective gas-temperature distribution (absolute minimum rotor coolant flow) exposes the turbine inner shrouds to the hottest gas layers, while the coolest region, in general, exists near the blade midspan position. For most cases of immediate interest, the gas temperature near the inner shroud is around 4000° R or higher, resulting in an extreme shroud-cooling problem. The corresponding

coolant-flow decrease compared with the uniform profile is about 20 percent. For a turbine-inlet temperature of 2600° R, this might be reflected into approximately a 1-percent saving in thrust and horsepower for turbojet and turboprop engines.

Lewis Flight Propulsion Laboratory
National Advisory Committee for Aeronautics
Cleveland, Ohio, July 20, 1955

3776

171

APPENDIX A

SYMBOLS

| | |
|----------|---|
| A | amplitude of cosine wave representing temperature profile, °R |
| A_m | cross-sectional metal area, sq ft |
| a_{cr} | critical velocity of sound, $\sqrt{\frac{2\gamma}{\gamma+1} gRT}$ |
| B | constant in eq. (9), °R |
| b | blade length or span, ft |
| C | constant |
| c | exponent (see eq. (26)) |
| c_p | specific heat at constant pressure, Btu/(lb)(°F) |
| F | function |
| f | function |
| f | function |
| g | acceleration due to gravity, 32.2 ft/sec ² |
| h_f | effective inside heat-transfer coefficient, Btu/(sec)(sq ft)(°F) |
| h_i | inside heat-transfer coefficient, Btu/(sec)(sq ft)(°F) |
| h_o | outside heat-transfer coefficient, Btu/(sec)(sq ft)(°F) |
| K | coolant-flow parameter, $[(1 + \lambda) c_p w_a] / h_o l_o b$ |
| l_i | inside perimeter of blade used for defining effective heat-transfer coefficient, ft |
| l_o | outside perimeter of blade, ft |
| n | number representing either 1 or 2 |
| Opt | optimum effective gas-temperature profile |
| Q | heat-transfer rate, Btu/sec |

| | |
|---|---|
| R | gas constant, 53.3 ft-lb/(lb)(°R) |
| r | radius |
| S | stress-ratio factor |
| T | static temperature, °R |
| T' | total temperature, °R |
| T'' | relative total temperature, °R |
| \bar{T} | average temperature, °R |
| U | blade speed, ft/sec |
| V | absolute velocity, ft/sec |
| W | relative velocity, ft/sec |
| w | weight flow, lb/sec |
| x | spanwise distance from blade root to any point on blade, ft |
| x* | x/b |
| α | flow angle measured from axial direction, deg |
| γ | ratio of specific heats |
| λ | cooling-effectiveness parameter, h_o/h_f |
| ρ | static density, lb/cu ft |
| ρ' | total density, lb/cu ft |
| σ | stress, psi |
|  | representing effective gas-temperature profile given by complete cycle of cosine wave |
|  | representing effective gas-temperature profile given by one-half cycle of cosine wave |

Subscripts:

a air

5776

CM-4 DAG

al allowable
av average
b blade
e effective
g gas
h hub
t tip
u tangential direction
un uniform
x axial direction
1 turbine inlet
2 turbine exit

APPENDIX B

PROOF THAT ALLOWABLE BLADE TEMPERATURE DISTRIBUTION RESULTS

IN ABSOLUTE MINIMUM COOLANT FLOW

5776 A direct method of minimizing the cooling-air weight flow while restraining the maximum blade temperature by the allowable blade temperature was not developed. However, a relatively simple indirect method suffices to prove that the blade temperature corresponding to the allowable blade temperature results in the maximum average effective gas temperature for a given cooling-air weight flow. This is equivalent to proving that the allowable blade temperature distribution results in the absolute minimum cooling-air weight flow for a given average effective gas temperature. This proof is derived in the subsequent paragraphs. Throughout the proof, the values of w_a , h_o , h_f , b , c_p , l_o , and $T'_{a,h}$ are held constant.

The heat flow through the differential surface element dx is given by the following three equations:

$$dQ = h_o l_o b (T_{g,e} - T_b) dx^* \quad (B1)$$

$$dQ = w_a c_p dT'_{a,t} \quad (B2)$$

and

$$dQ = h_f l_o b (T_b - T'_{a,t}) dx^* \quad (B3)$$

Equations (B1) and (B2) may be integrated over the entire blade span to give

$$\frac{Q}{h_o l_o b} = \int_0^1 T_{g,e} dx^* - \int_0^1 T_b dx^* = \bar{T}_{g,e} - \bar{T}_b \quad (B4)$$

and

$$\frac{Q}{w_a c_p} = T'_{a,t} - T'_{a,h} \quad (B5)$$

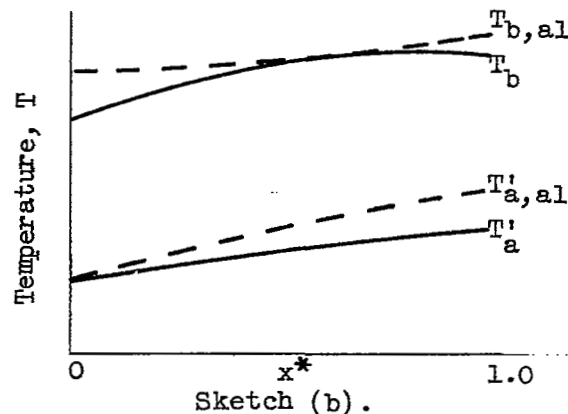
If equation (B4) is rewritten as

$$\bar{T}_{g,e} = \frac{Q}{h_o l_o b} + \bar{T}_b \quad (B6)$$

it is clear that the average effective gas temperature $\bar{T}_{g,e}$ can be increased by increasing the average blade temperature \bar{T}_b , provided the total heat-flow rate Q does not decrease. It will be proved that Q does not decrease as \bar{T}_b is increased.

The maximum average blade temperature subject to the restraint that the blade temperature cannot exceed the allowable blade temperature corresponds to the average allowable blade temperature. It must be proved that as \bar{T}_b is increased to $\bar{T}_{b,al}$ the value of Q is not decreased. Since $T'_{a,h}$ is constant, equation (B5) shows that Q decreases only if $T'_{a,t}$ decreases. Thus, the problem is reduced to proving that $T'_{a,t}$ does not decrease as \bar{T}_b increases.

Consider a comparison of the cooling-air temperature distributions for $\bar{T}_b < \bar{T}_{b,al}$, except at a finite number of tangency points, and $\bar{T}_b = \bar{T}_{b,al}$. These distributions are illustrated for a particular case in sketch (b), where $T'_{a,al}$ is associated with $\bar{T}_{b,al}$. In this sketch, $T'_{a,al}$ is arbitrarily drawn to exceed T'_a at all spanwise positions:



If equations (B2) and (B3) are combined, the slope of the temperature distribution curve can be expressed by

$$\frac{dT'_a}{dx^*} = \frac{h_F l_o b}{w_a c_p} (T_b - T'_a) \quad (B7)$$

From equation (B7) and the sketch (b), the rate of change of the cooling-air temperature at $x^* = 0$ is greater for $\bar{T}_b = \bar{T}_{b,al}$ than for $\bar{T}_b < \bar{T}_{b,al}$. (In the event that a tangency point exists at $x^* = 0$, the rates of change in the temperatures are identical. However, the argument

may be pursued by proceeding to a spanwise position immediately beyond $x^* = 0$.) Thus, in the neighborhood of the blade root, $T'_{a,a1} > T'_a$, as shown in sketch (b). If the cooling-air temperature at the tip is less for $\bar{T}_b = \bar{T}_{b,a1}$ than for $\bar{T}_b < \bar{T}_{b,a1}$ (i.e., $T'_{a,a1} < T'_a$), it is clear that the corresponding curves of the cooling-air temperature distributions must cross at some spanwise position. If this occurs, it is necessary that at the intersection point $T'_{a,a1} = T'_a$ and $\frac{dT'_{a,a1}}{dx^*} < \frac{dT'_a}{dx^*}$. However, equation (B7) shows that these conditions are incompatible if $\bar{T}_b \leq \bar{T}_{b,a1}$. Thus, the cooling-air temperature at the blade tip cannot decrease as \bar{T}_b is increased to $\bar{T}_{b,a1}$. This completes the proof, since this implies that Q does not decrease and therefore $\bar{T}_{g,e}$ must increase.

APPENDIX C

EVALUATION OF RELATION BETWEEN EFFECTIVE GAS AND
TURBINE-INLET TEMPERATURES

The difference between the total absolute and relative gas temperatures at the turbine inlet as given by the energy equation is

$$T_1' - T_1'' = \frac{v_1^2 - w_1^2}{2gJc_p} = \frac{\gamma - 1}{2g\gamma R} (v_1^2 - w_1^2) \quad (C1)$$

Taking the difference between equation (C1) applied at hub section and applied at any spanwise position gives

$$(T_1' - T_1'') - (T_{1,h}' - T_{1,h}'') = \frac{\gamma - 1}{2g\gamma R} (v_1^2 - w_1^2 - v_{1,h}^2 + w_{1,h}^2) \quad (C2)$$

For free-vortex flow at the turbine inlet, the velocities at different radial positions are related by the equations

$$\left. \begin{aligned} \frac{U}{U_h} &= \frac{r}{r_h} \\ \frac{V_{1,u}}{V_{1,u,h}} &= \frac{r_h}{r} \\ V_{1,x,h} &= V_{1,x} = W_{1,x,h} = W_{1,x} \end{aligned} \right\} \quad (C3)$$

Employing the last expression and the equations

$$v_1^2 = v_{1,x}^2 + v_{1,u}^2$$

$$w_1^2 = w_{1,x}^2 + w_{1,u}^2$$

equation (C2) becomes

$$(T_1' - T_1'') - (T_{1,h}' - T_{1,h}'') = \frac{\gamma - 1}{2g\gamma R} (v_{1,u}^2 - v_{1,u,h}^2 - w_{1,u}^2 + w_{1,u,h}^2) \quad (C4)$$

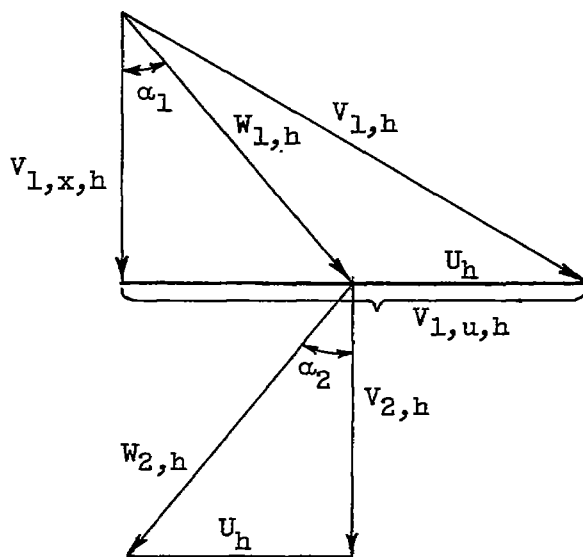
Furthermore, if $w_{1,u}$ is replaced by its equivalent $(v_{1,u} - U)$, equation (C4) becomes

$$(T_1' - T_1'') - (T_{1,h}' - T_{1,h}'') = \frac{\gamma - 1}{2\gamma R} (U_h^2 - U^2 + 2UV_{1,u} - 2U_h V_{1,u,h})$$

or, using equation (C3) and the condition $U_h^2 = U_t^2 \left(\frac{r_h}{r_t}\right)^2$,

$$(T_1' - T_1'') - (T_{1,h}' - T_{1,h}'') = \frac{\gamma - 1}{2\gamma R} U_t^2 \left(\frac{r_h}{r_t}\right)^2 \left[1 - \left(\frac{r}{r_h}\right)^2 \right] \quad (C5)$$

Equation (C5) relates the difference between the total absolute and relative gas temperatures at any spanwise position to the value at the turbine hub. The value of this difference at the hub section can now be related to the turbine blade tip speed and hub-tip radius ratio for impulse conditions with no exit whirl if losses are neglected. This relation will now be determined, since these assumptions are reasonable for the purpose of this report. For such conditions, the turbine velocity diagram at the hub can be represented as in sketch (c). In this case, $\alpha_1 = \alpha_2$:



Sketch (c).

Since

$$\begin{aligned} V_{1,h}^2 &= V_{1,x,h}^2 + V_{1,u,h}^2 = (W_{1,h}^2 - U_h^2) + (2U_h)^2 \\ &= W_{1,h}^2 + 3U_h^2 \end{aligned}$$

equation (C1) applied at the hub gives

$$T'_{1,h} - T''_{1,h} = \frac{3(\gamma-1)U_h^2}{2\gamma R} = \frac{3(\gamma-1)U_t^2}{2\gamma R} \left(\frac{r_h}{r_t}\right)^2 \quad (C6)$$

If equation (C6) is introduced into equation (C5), the temperature difference at any spanwise position becomes

$$T'_1 - T''_1 = \frac{\gamma-1}{2\gamma R} U_t^2 \left(\frac{r_h}{r_t}\right)^2 \left[4 - \left(\frac{r}{r_t}\right)^2 \right] \quad (C7)$$

Introducing the radial position x^* as given by

$$x^* = \frac{r - r_h}{r_t - r_h}$$

this expression becomes

$$T'_1 - T''_1 = \frac{\gamma-1}{2\gamma R} U_t^2 \left(\frac{r_h}{r_t}\right)^2 \left\{ 4 - \left[1 + x^* \left(\frac{r_t}{r_h} - 1\right) \right]^2 \right\} \quad (C8)$$

Equation (C8) expresses the difference between the total absolute and relative gas temperatures at any spanwise position in terms of only the turbine tip speed and hub-tip radius ratio. The average difference between these temperatures can be obtained by integrating equation (C8). The average difference weighted according to the annular area and therefore weight flow per uniform specific weight flow is

$$(T'_1 - T''_1)_{av} = \frac{2b}{r_t^2 - r_h^2} \int_0^1 r(T'_1 - T''_1) dx^*$$

or

$$(T'_1 - T''_1)_{av} = \frac{(\gamma-1)b r_h U_t^2 \left(\frac{r_h}{r_t}\right)^2}{\gamma R (r_t^2 - r_h^2)} \int_0^1 \left[1 + x^* \left(\frac{r_t}{r_h} - 1\right) \right] \left\{ 4 - \left[1 + x^* \left(\frac{r_t}{r_h} - 1\right) \right]^2 \right\} dx^* \quad (C9)$$

Upon integration, this expression reduces to

$$(T_1' - T_1'')_{av} = \frac{\gamma - 1}{4\gamma R} U_t^2 \left(\frac{r_h}{r_t}\right)^2 \left[7 - \left(\frac{r_t}{r_h}\right)^2 \right] \quad (C10)$$

If it is finally assumed that the total relative temperature is equal to the effective gas temperature, equations (C8) and (C10) become

$$T_1' - T_{g,e} = \frac{\gamma - 1}{2\gamma R} U_t^2 \left(\frac{r_h}{r_t}\right)^2 \left\{ 4 - \left[1 + x^* \left(\frac{r_t}{r_h} - 1\right) \right]^2 \right\} \quad (27)$$

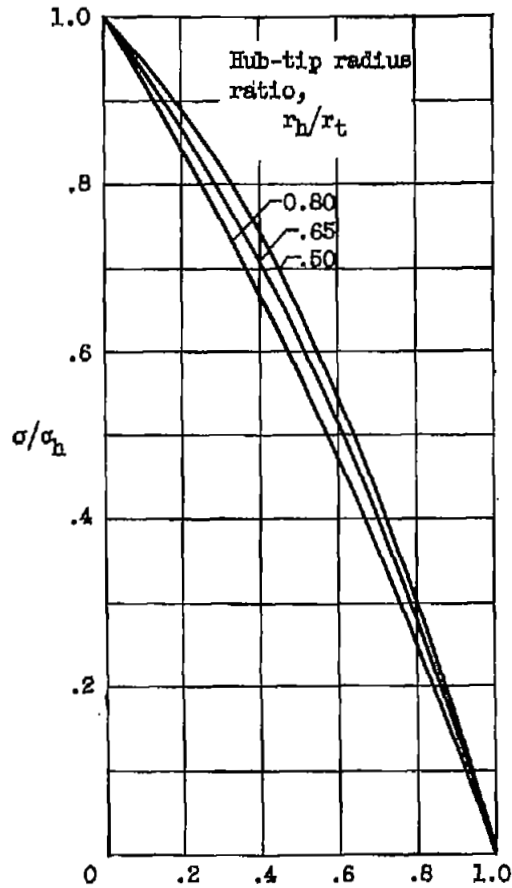
and

$$\bar{T}_1' - \bar{T}_{g,e} = \frac{\gamma - 1}{4\gamma R} U_t^2 \left(\frac{r_h}{r_t}\right)^2 \left[7 - \left(\frac{r_t}{r_h}\right)^2 \right] \quad (28)$$

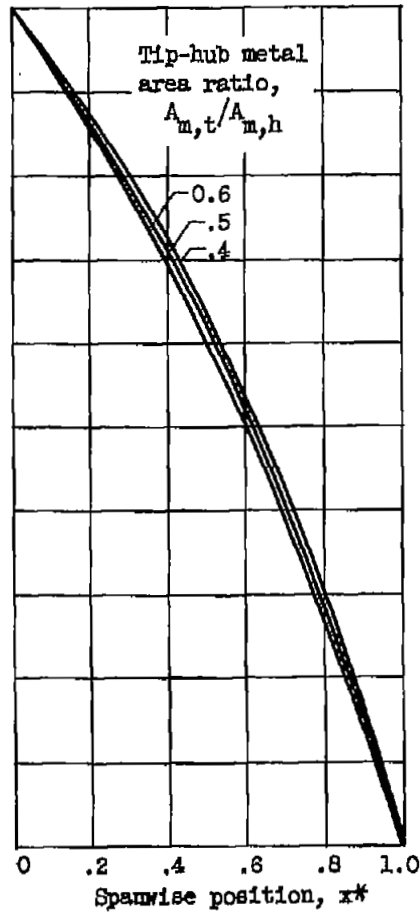
REFERENCES

1. Ziemer, Robert R., and Slone, Henry O.: Analytical Procedures for Rapid Selection of Coolant Passage Configurations for Air-Cooled Turbine Rotor Blades and for Evaluation of Heat-Transfer, Strength, and Pressure-Loss Characteristics. NACA RM E52G18, 1952.
2. Slone, Henry O., Hubbartt, James E., and Arne, Vernon L.: Method of Designing Corrugated Surfaces Having Maximum Cooling Effectiveness within Pressure-Drop Limitations for Application to Cooled Turbine Blades. NACA RM E54H20, 1954.
3. Norgren, Carl T., and Childs, J. Howard: Effect of Liner Air-Entry Holes, Fuel State, and Combustor Size on Performance of an Annular Turbojet Combustor at Low Pressures and High Air-Flow Rates. NACA RM E52J09, 1953.
4. Farmer, J. Elmo: Relation of Nozzle-Blade and Turbine-Bucket Temperatures to Gas Temperatures in a Turbojet Engine. NACA RM E7L12, 1948.
5. Mark, Herman, and Zettle, Eugene V.: Effect of Air Distribution on Radial Temperature Distribution of One-Sixth Sector of Annular Turbojet Combustor. NACA RM E9I22, 1950.
6. Moseson, Merland L., Krasner, Morton H., and Ziemer, Robert R.: Mechanical Design Analysis of Several Noncritical Air-Cooled Turbine Disks and a Corrugated-Insert Air-Cooled Turbine Rotor Blade. NACA RM E53E21, 1953.

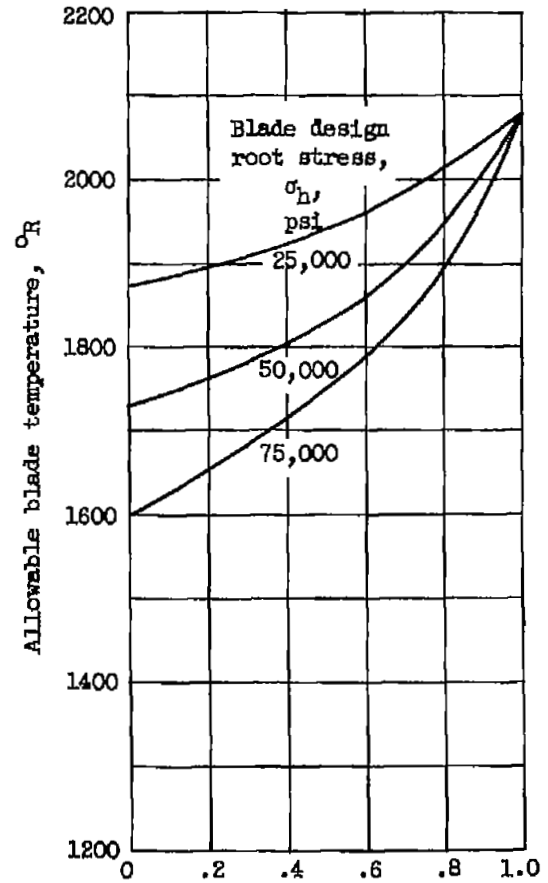
7. Slone, Henry O., and Hubbartt, James E.: Analysis of Factors Affecting Selection and Design of Air-Cooled Single-Stage Turbines for Turbojet Engines. IV - Coolant-Flow Requirements and Performance of Engines Using Air-Cooled Corrugated-Insert Blades. NACA RM E55C09, 1955.
8. Esgar, Jack B., and Ziemer, Robert R.: Effect of Turbine Cooling with Compressor Air Bleed on Gas-Turbine Engine Performance. NACA RM E54L20, 1955.



(a) Stress distribution for various turbine hub-tip radius ratios;
 $A_{m,t}/A_{m,h} = 0.5$.

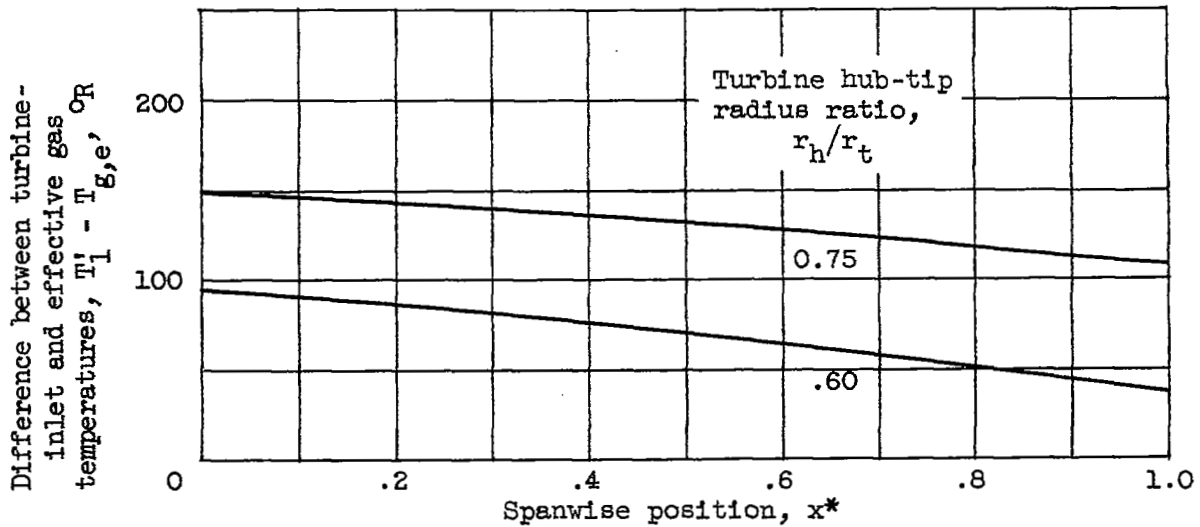


(b) Stress distribution for various blade metal tapers;
 $r_h/r_t = 0.65$.

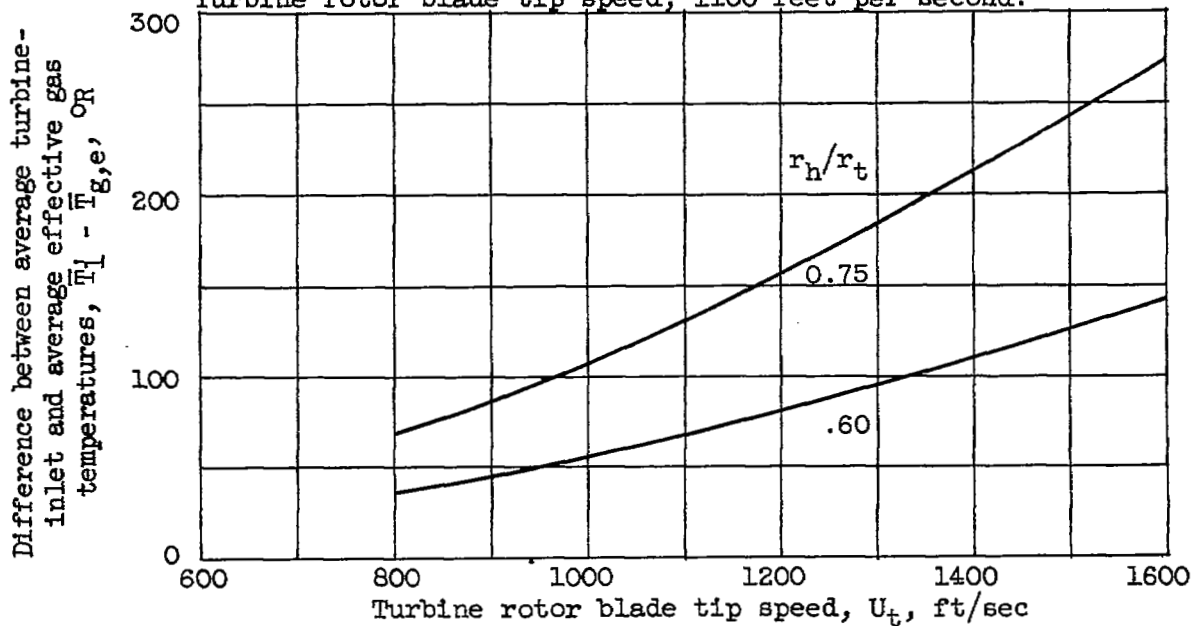


(c) Allowable blade temperature distributions for three design stresses. Material, A-286.

Figure 1. - Spanwise distribution of stress and allowable blade temperature.



(a) Difference between turbine-inlet and effective gas temperature at each spanwise position for representative conditions. Turbine rotor blade tip speed, 1100 feet per second.



(b) Difference between average turbine-inlet and average effective gas temperatures for range of tip speeds.

Figure 2. - Difference between turbine-inlet and rotor effective gas temperatures for free-vortex design with impulse conditions at root and no losses.

3776

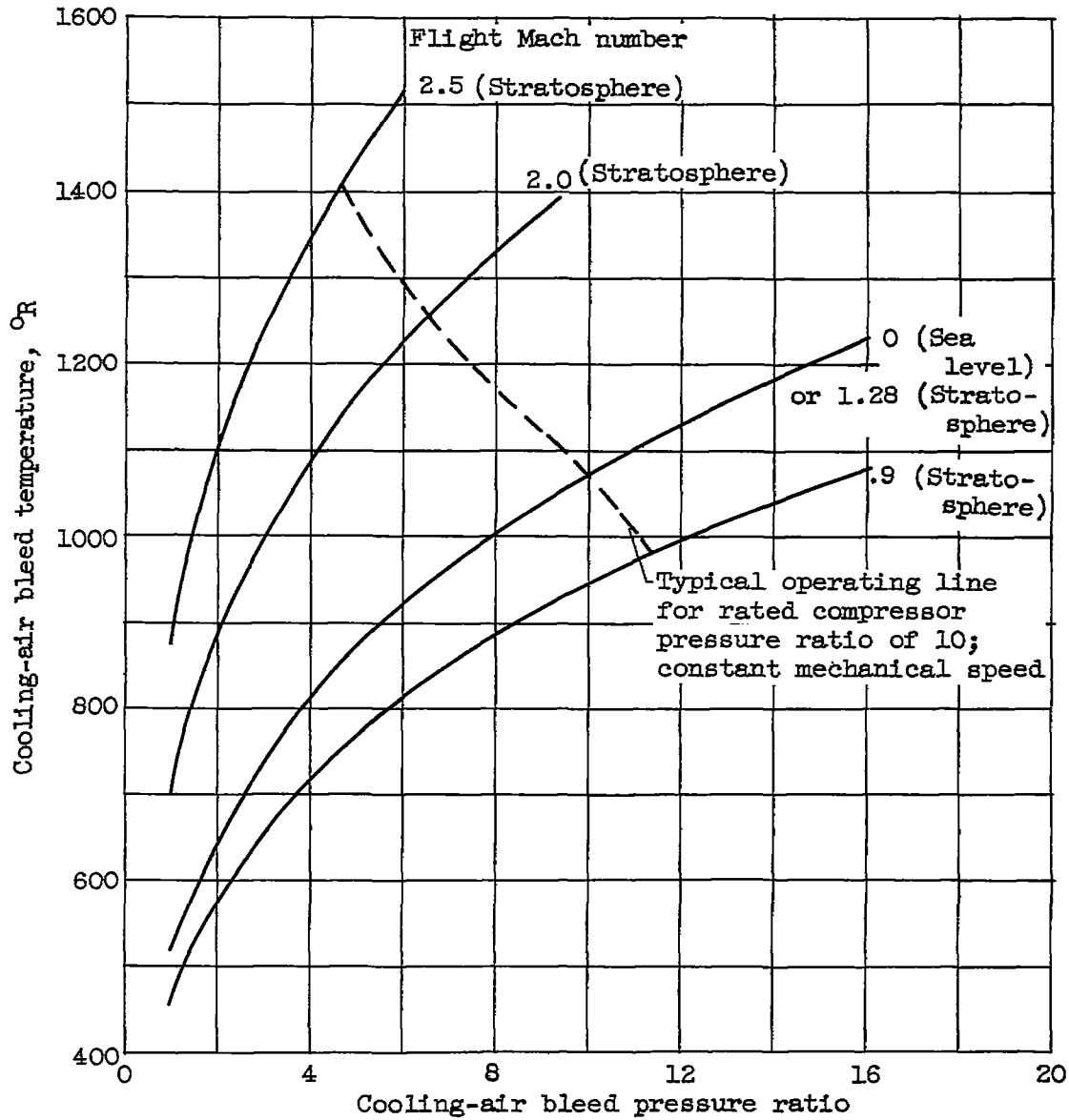


Figure 3. - Variation of cooling-air bleed temperature with bleed pressure ratio and flight speed.

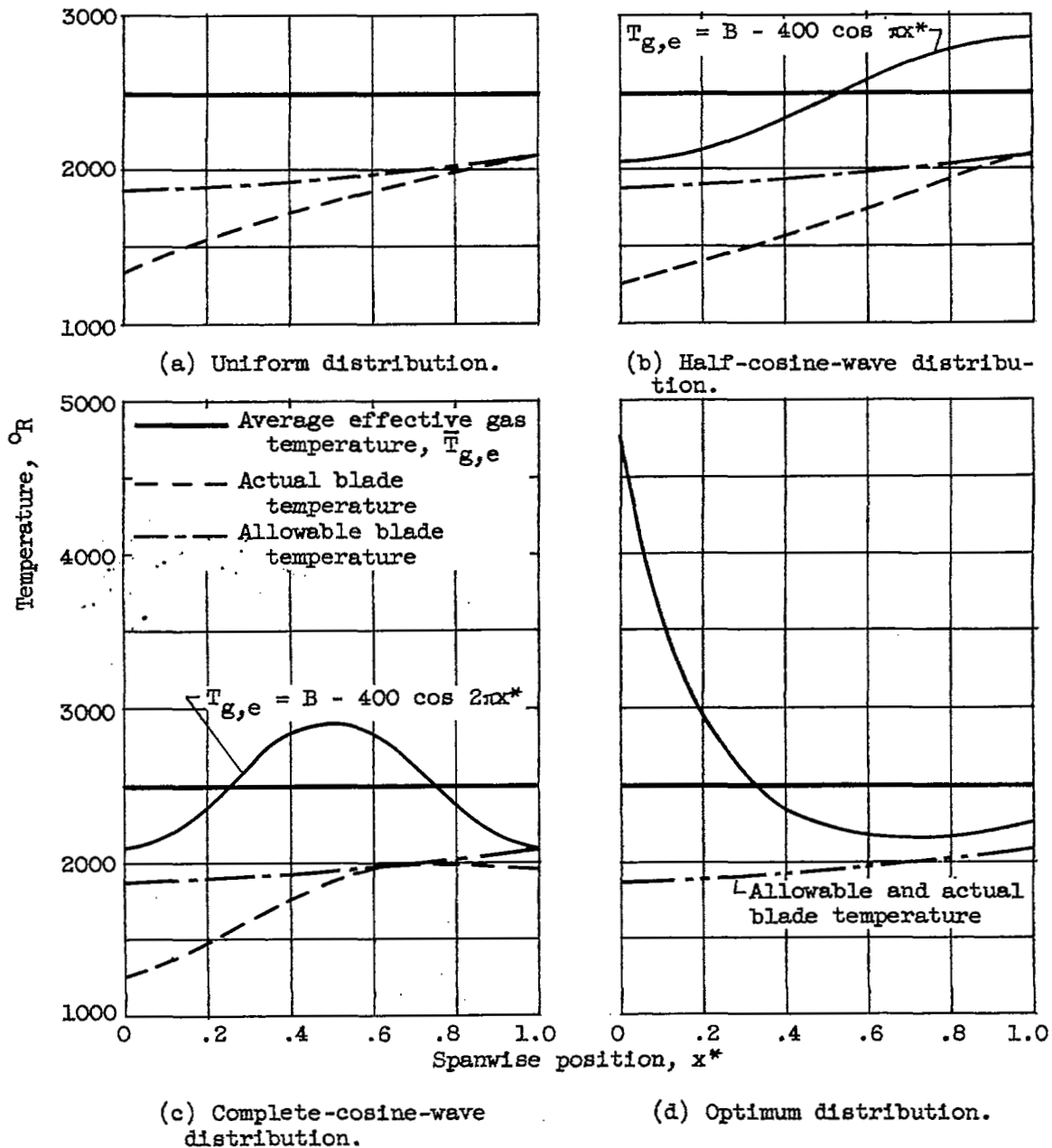


Figure 4. - Spanwise temperature distributions for four effective gas-temperature profiles. Cooling-effectiveness parameter, 0.30; blade design root stress, 25,000 psi; blade-inlet cooling-air temperature, 1000° R.

3776

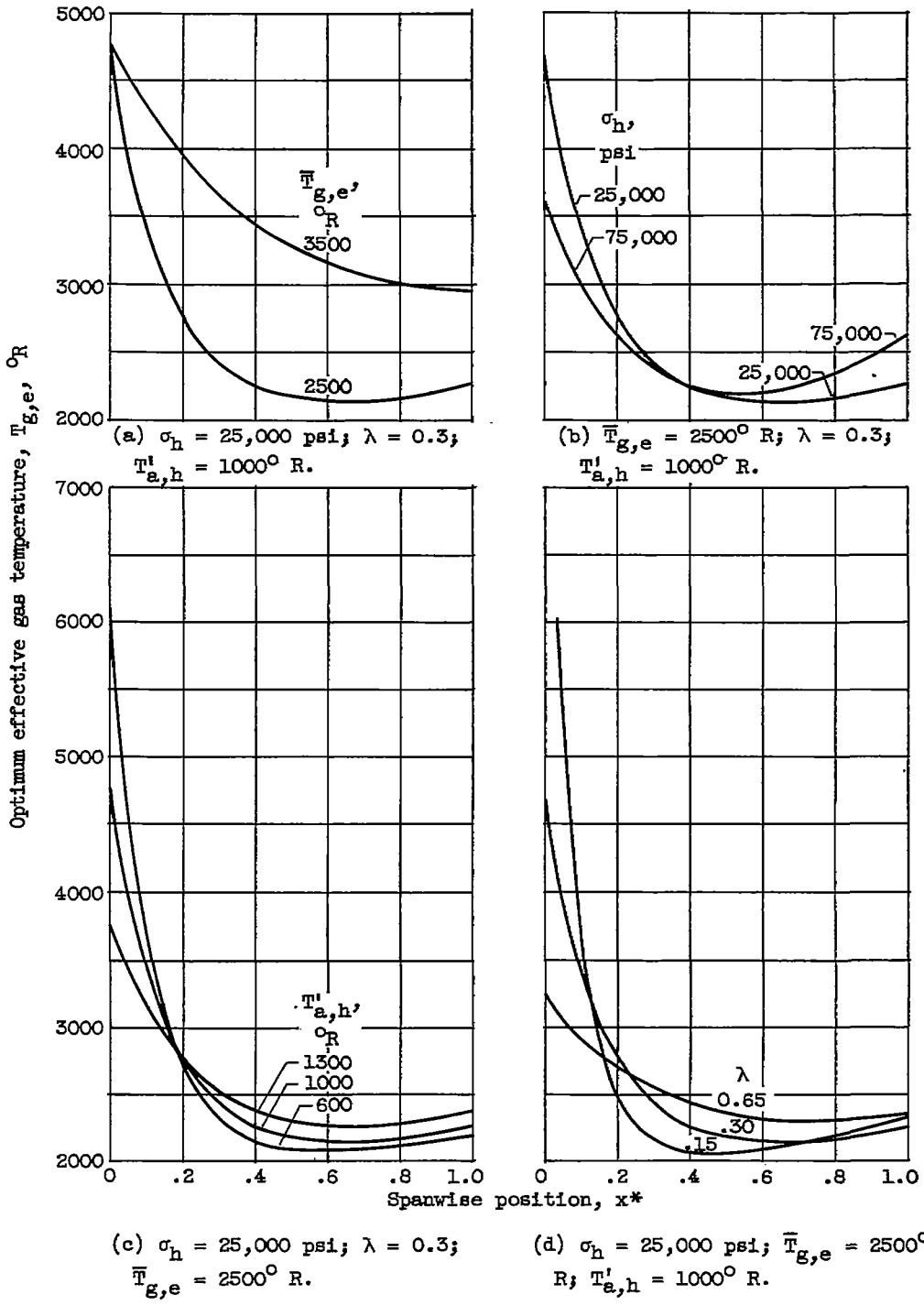
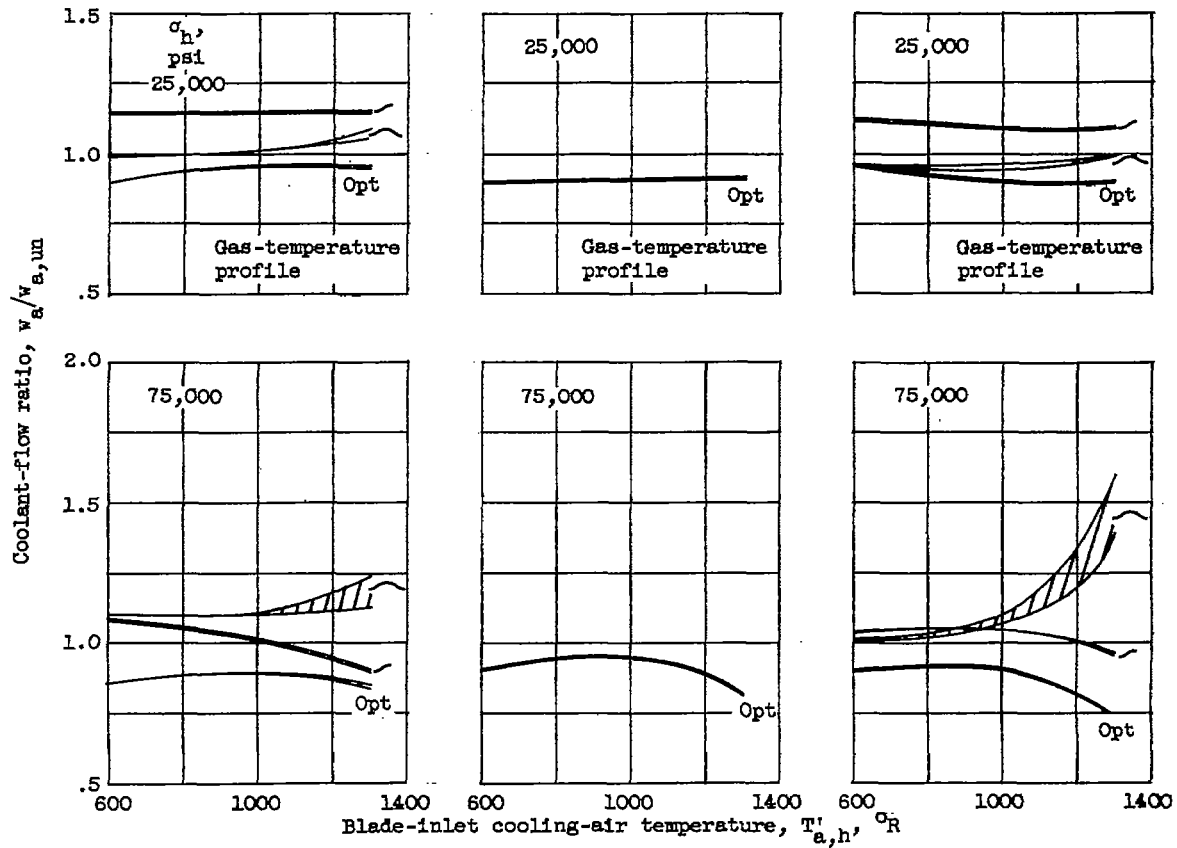
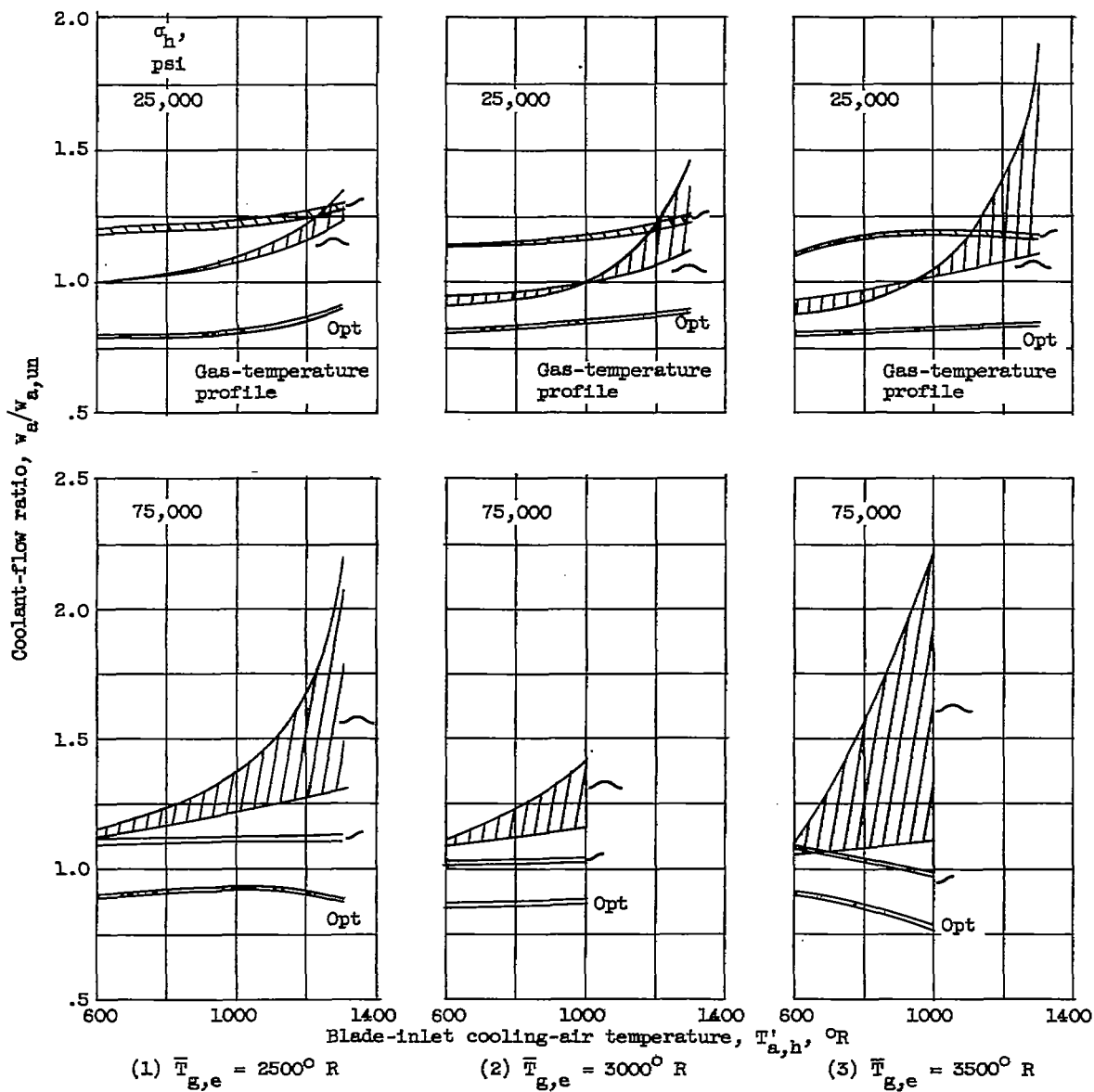


Figure 5. - Effect of cooling conditions and blade cooling effectiveness on optimum effective gas-temperature profile.

(1) $\bar{T}_{g,e} = 2500^{\circ} \text{R}$ (2) $\bar{T}_{g,e} = 3000^{\circ} \text{R}$ (3) $\bar{T}_{g,e} = 3500^{\circ} \text{R}$

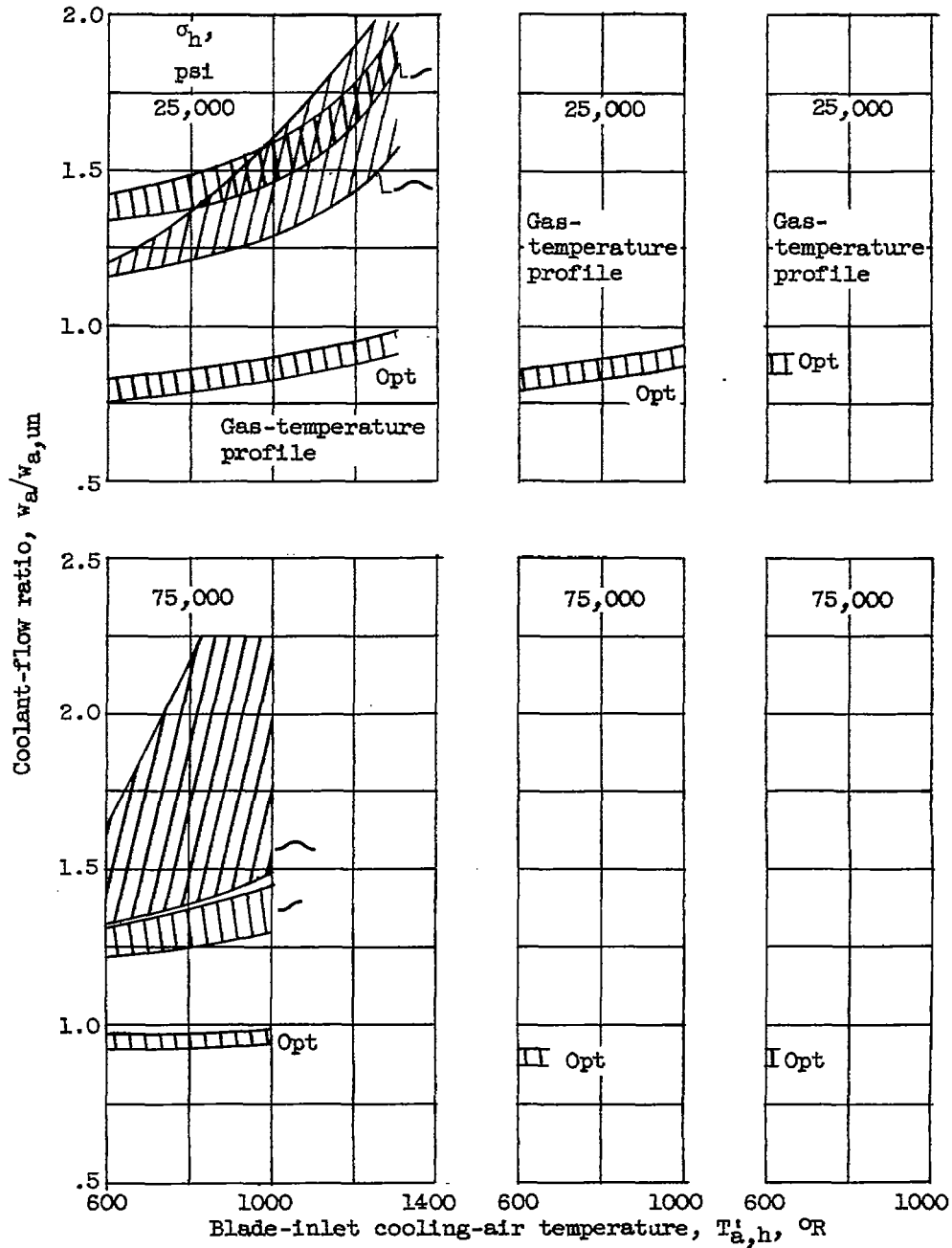
(a) Cooling-effectiveness parameter, 0.15.

Figure 6. - Effect of design variables on ratio of coolant flow for each effective gas-temperature profile to that for uniform profile. Cosine-wave amplitude, 400°R .



(b) Cooling-effectiveness parameter, 0.30.

Figure 6. - Continued. Effect of design variables on ratio of coolant flow for each effective gas-temperature profile to that for uniform profile. Cosine-wave amplitude, 400° R .



(1) $\bar{T}_{g,e} = 2500^\circ \text{R}$ (2) $\bar{T}_{g,e} = 3000^\circ \text{R}$ (3) $\bar{T}_{g,e} = 3500^\circ \text{R}$

(c) Cooling-effectiveness parameter, 0.65.

Figure 6. - Concluded. Effect of design variables on ratio of coolant flow for each effective gas-temperature profile to that for uniform profile. Cosine-wave amplitude, 400°R .

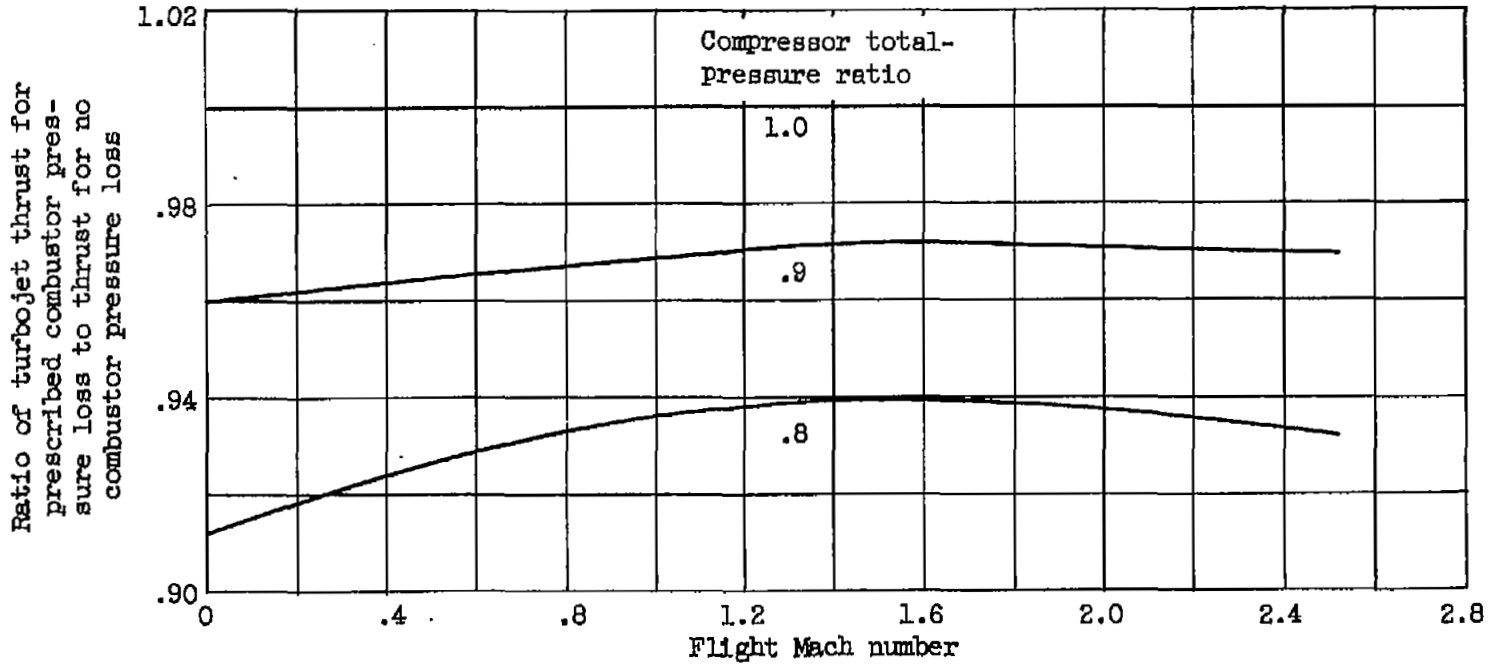


Figure 7. - Effect of combustor pressure loss on turbojet-engine thrust for typical engine operating line given in figure 5. Rated compressor pressure ratio, 10.

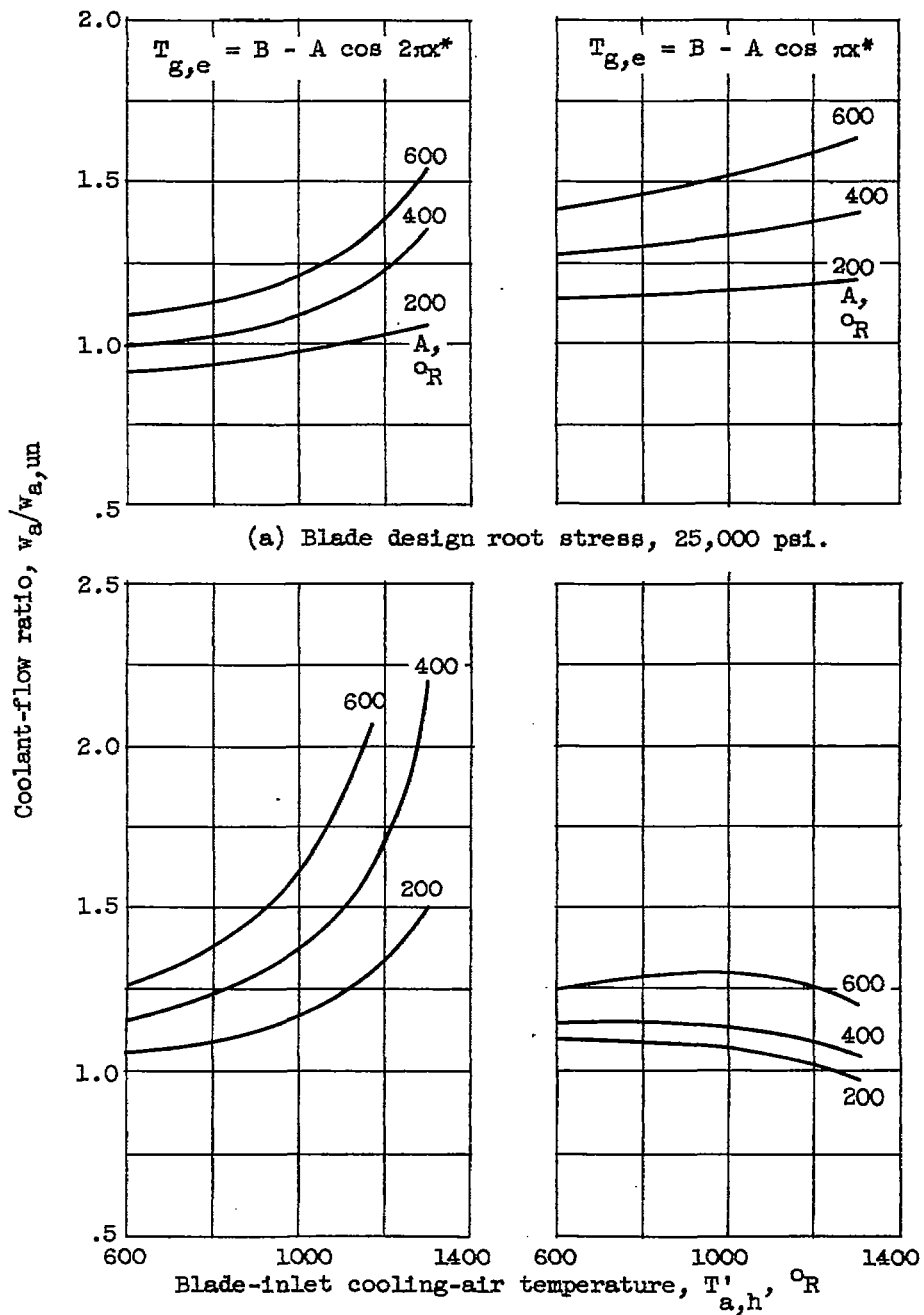


Figure 8. - Effect of cosine-wave amplitude on cooling-air requirements for temperature profiles representable by cosine wave. Laminar cooling-air flow; average effective gas temperature, 2500°R ; cooling-effectiveness parameter, 0.30.

NASA Technical Library



3 1176 01436 5036

